1979

Pulsed Doppler imaging of the carotid bifurcation

Richard Dean Miles
Iowa State University

INFORMATION TO USERS

This was produced from a copy of a document sent to us for microfilming. While the most advanced technological means to photograph and reproduce this document have been used, the quality is heavily dependent upon the quality of the material submitted.

The following explanation of techniques is provided to help you understand markings or notations which may appear on this reproduction.

1. The sign or "target" for pages apparently lacking from the document photographed is "Missing Page(s)". If it was possible to obtain the missing page(s) or section, they are spliced into the film along with adjacent pages. This may have necessitated cutting through an image and duplicating adjacent pages to assure you of complete continuity.

2. When an image on the film is obliterated with a round black mark it is an indication that the film inspector noticed either blurred copy because of movement during exposure, or duplicate copy. Unless we meant to delete copyrighted materials that should not have been filmed, you will find a good image of the page in the adjacent frame.

3. When a map, drawing or chart, etc., is part of the material being photographed the photographer has followed a definite method in "sectioning" the material. It is customary to begin filming at the upper left hand corner of a large sheet and to continue from left to right in equal sections with small overlaps. If necessary, sectioning is continued again—beginning below the first row and continuing on until complete.

4. For any illustrations that cannot be reproduced satisfactorily by xerography, photographic prints can be purchased at additional cost and tipped into your xerographic copy. Requests can be made to our Dissertations Customer Services Department.

5. Some pages in any document may have indistinct print. In all cases we have filmed the best available copy.

University
Microfilms
International

300 N. ZEEB ROAD, ANN ARBOR, MI 48106
18 BEDFORD ROW, LONDON WC1R 4EJ, ENGLAND

PLEASE NOTE:

In all cases this material has been filmed in the best possible way from the available copy. Problems encountered with this document have been identified here with a check mark ✓.

1. Glossy photographs ✓
2. Colored illustrations _____
3. Photographs with dark background ✓
4. Illustrations are poor copy _____
5. Print shows through as there is text on both sides of page _____
6. Indistinct, broken or small print on several pages _____ throughout _____
7. Tightly bound copy with print lost in spine _____
8. Computer printout pages with indistinct print _____
9. Page(s) _____ lacking when material received, and not available from school or author _____.
10. Page(s) _____ seem to be missing in numbering only as text follows _____
11. Poor carbon copy _____
12. Not original copy, several pages with blurred type _____
13. Appendix pages are poor copy _____
14. Original copy with light type _____
15. Curling and wrinkled pages _____
16. Other _____

Pulsed Doppler imaging of the carotid bifurcation

by

Richard Dean Miles

A Dissertation Submitted to the

Graduate Faculty in Partial Fulfillment of

The Requirements for the Degree of

DOCTOR OF PHILOSOPHY

Co-majors: Biomedical Engineering
Electrical Engineering

Approved:

Signature was redacted for privacy.

Signature was redacted for privacy.

In Charge of Major Work

Signature was redacted for privacy.

Professor-in-charge,
Program in Biomedical Engineering

Signature was redacted for privacy.

For the Major Department

Signature was redacted for privacy.

For the Graduate College

Iowa State University
Ames, Iowa

1979

TABLE OF CONTENTS

INTRODUCTION

Stroke is a leading cause of cardiovascular morbidity and mortality, killing nearly 250,000 and disabling another 350,000 people in the United States every year. Fifty percent of the strokes are the result of atherosclerotic occlusive disease of the carotid arteries which supply blood to the brain. The carotids are susceptible to occlusive plaque formation in localized regions of the vessel, especially at the carotid bifurcation. These plaques may grow in size until they reduce the blood flow to the brain or until they break off, travel to the brain, and cause a catastrophic stroke. Fortunately, the occlusive plaques can be surgically removed to restore cerebral blood flow.

X-ray angiography is the standard diagnostic procedure used to evaluate patients with suspected carotid occlusive disease. This requires the injection of a radiopaque dye into the cerebral circulation. Since X-rays are blocked by the dye, the X-ray films show a morphological outline of the vessel including any vessel obstructions. By changing the position of the patient, either lateral, anterior-posterior (A-P) or oblique arterial outlines can be obtained. These multiple views can be used to determine the degree of vessel obstruction. This procedure remains the "gold standard"; unfortunately, it poses a definite risk for the patient. The X-ray angiographic procedure may precipitate a stroke resulting in death or permanent disability for the patient. For this reason, the physician is reluctant to use angiography for routine screening and follow-up of patients with suspected atherosclerotic occlusive disease.

As an alternate procedure, ultrasonic arteriography can be used to non-invasively create images of the carotid arteries. This procedure uses harmless Doppler ultrasound to detect blood flow and a cathode ray tube to store two-dimensional images of the carotid arteries. The ultrasonic-produced images are similar to lateral views obtained with X-ray angiography.

Because of the detailed images and the insurance of patient safety, ultrasonic arteriography is used for the initial screening and surgical follow-up of patients with carotid artery disease. Unfortunately, the arterial image obtained is only two-dimensional. Thus, when a two-dimensional image is used to estimate the size of a three-dimensional stenosis, a significant error may result. This error could be reduced substantially if images with three dimensions could be made with ultrasonic arteriography.

This dissertation describes a microcomputer-aided ultrasonic arteriograph (UA) which was designed to draw orthogonal projections of the carotid arteries on a video screen. Flow and position information generated during an ultrasonic examination are input to a microcomputer which analyzes the data and produces a vessel image. The image is produced during the examination and consists of a plane view at the top of the screen and a depth view at the bottom of the screen. The two views are projections of the vessel on orthogonal planes and therefore contain information in three dimensions. Since the two views are produced simultaneously, the term "three-dimensional" will be used to describe the vessel image. Simultaneous ultrasonic imaging in three dimensions

represents a significant new technique which will help the physician to better estimate the degree of arterial constriction caused by a stenosis. Moreover, the number of ultrasonic false positive and false negative arterial examinations will be reduced when multiple views are used for diagnosis.

At this point in the discussion, let us examine the anatomy of the cerebrovascular system and the disease process which causes arterial stenoses.

Anatomy

The cerebrovasculature begins at the arch of the aorta where the brachial cephalic, left common carotid and left subclavian arteries originate (see Figure 1). The brachiocephalic artery subdivides to form the right subclavian and right common carotid arteries. The subclavian artery supplies the upper extremity and gives one important branch, the vertebral artery to the brain.

Each common carotid artery passes up the neck beside the trachea and divides into the external and internal carotid arteries at the upper level of the thyroid cartilage. The inside diameter (I.D.) of the common carotid artery in a normal adult male is a nominal 8 mm, the internal carotid I.D. is a nominal 5 mm and the external carotid I.D. is a nominal 4 mm. The carotid sinus is a dilation of the terminal portion of the common carotid and the beginning of the internal carotid. Its walls are quite elastic and the sensory nerve endings from this region are part of the blood pressure and respiratory regulating mechanisms.

The external carotid supplies the structures in the neck, face, mouth, jaws and scalp. Its branches are the superior thyroid, lingual, facial, occipital, posterior auricular, ascending pharyngeal, superficial temporal, and maxillary arteries.

The internal carotid enters the middle cranial fossa through the carotid canal where it helps to form the arterial circle at the base of the brain. The internal carotid gives off no branches in the neck.

The vertebral arteries pass up through the lateral foramina of the cervical vertebrae and through the foramen magnum into the cranial cavity. On the upper surface of the brain stem, the two vertebral arteries unite to form the basilar artery which continues into the middle cranial fossa. The two internal carotids and the basilar artery form an arterial circle at the base of the brain (circle of Willis). From these vessels arise the arteries supplying the brain. The anterior and middle cerebral arteries are branches of the internal carotid; the posterior cerebral artery is a branch of the basilar artery. The ophthalmic artery supplying the eyeball and forehead also come from the internal carotid.

Atherosclerotic occlusive disease

Atherosclerotic occlusive disease is a lifelong process affecting localized regions of the arterial tree. Atherosclerotic lesions are often found at branches, bifurcations and in curved segments of arteries. These lesions can begin in childhood as fatty deposits of cholesterol and other lipid materials in the arterial walls.

Figure 1. Anatomy of the cerebrovascular system

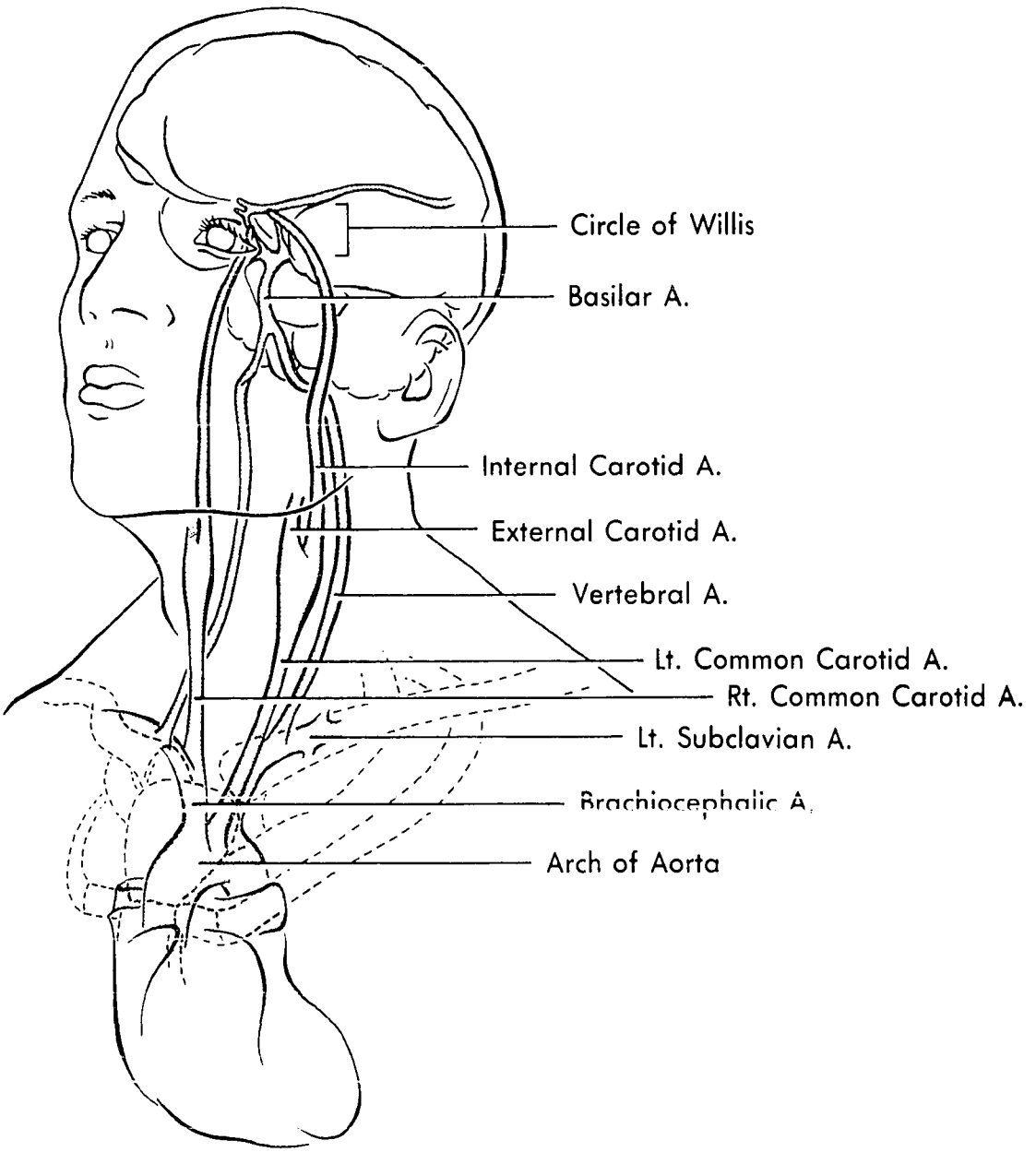
Circle of Willis
Basilar A.
Internal Carotid A.
External Carotid A.
Vertebral A.
Lt. Common Carotid A.
Rt. Common Carotid A.
Lt. Subclavian A.
Brachiocephalic A.
Arch of Aorta

After observing that particular arterial regions are more susceptible to occlusive disease, Fry (1969) and Caro et al. (1971) proposed that blood flow conditions cause the initiation and progression of atherosclerotic lesions. Fry proposes that in certain regions of the arterial tree, shear forces are great enough to cause injury to the endothelial lining of the artery. He goes on to say that these regions of high shear may increase cholesterol diffusion into the wall and promote the production of thrombi. Caro presents an opposing theory. He suggests that in vessel regions where there are stagnation zones, the wall shear force is low. The low shear force causes a reduction in the arterial wall-to-blood transport of cholesterol and other wall-produced lipids. Instead of being carried away by the blood, the materials accumulate in the arterial walls causing atherosclerotic lesions.

Because of the long-term development of lesions and the difficulty of measuring wall shear stress, neither Caro's or Fry's theory can be proved. However, it is known that these wall deposits eventually harden, thereby reducing the natural elasticity of the arterial walls. This process, called "hardening of the arteries," also promotes the entrapment and deposition of platelets, erythrocytes, calcium, lipids and other materials carried by the blood. These trapped materials accumulate and reduce the size of the arterial lumen, sometimes breaking off and traveling to the brain where they may produce a stroke. Plaques may grow in size until they reduce the blood flow to the brain. Tsai et al. (1971) experimentally determined that blood flow through an artery is

not reduced substantially until approximately 85 percent of the lumen area is occluded. Thus, a fairly tight stenosis must be present before blood flow through a vessel is substantially reduced.

The carotid arteries have been shown to normally carry 85 to 90 percent of the blood flowing to the brain, while the two vertebral arteries carry the remainder (Roberts et al. 1964). However, if one of the carotids becomes totally occluded, the other carotid and the vertebrals may be able to carry most of the necessary cerebral blood flow.

Severe occlusions of the common or internal carotid arteries often cause reduced blood flow to the brain resulting in ischemia. Patients with ischemia may complain of dizziness, fainting, confusion, blurred vision, weakness of facial muscles, slurred speech or a myriad of other symptoms (Thompson 1975). Patients with these symptoms are generally referred to a vascular clinic for examination and diagnosis. The vascular examination generally includes a complete patient history and physical along with a series of non-invasive hemodynamic tests.

This project concerns itself with one diagnostic instrument used in the evaluation of patients with suspected occlusive disease of the carotid arteries. The instrument, a Hokanson Ultrasonic Arteriograph[1], is used to non-invasively image blood flow in the carotid arteries. This instrument uses pulsed-Doppler ultrasound to detect blood flow, a

---

[1]A pulsed-Doppler ultrasonic arteriograph (UA) was manufactured by D. E. Hokanson of Seattle, Washington in 1976 for use in the vascular laboratory of Southern Illinois University School of Medicine in Springfield, Illinois. Modifications and improvements in the imaging capabilities of this instrument are the basis for this project.

transducer positioning arm to generate transducer coordinates and a bistable storage oscilloscope to store an image of the lumen of the carotid artery under examination. The image is created by passing the transducer back and forth across the patient's neck over the region of the carotid bifurcation (see Figure 2). Whenever flow is detected under the transducer, a small dot is placed on the oscilloscope screen. Repeated passings of the transducer across the neck creates a group of closely spaced dots which coalesce to form an image of the arterial lumen. The anatomical position of the bifurcation varies between individuals so the ultrasonic examiner must start low on the neck to first locate the common carotid. By following and imaging this vessel anteriorly, the bifurcation can be located, after which the examiner continues to image the internal and external carotid branches to the level of the mandible. The image is similar to a lateral view obtained with radiographic angiography. Arterial occlusive disease shows up as narrowed regions in the vessel image. The examiner takes a Polaroid photograph of the display screen to create a permanent copy for later reference by the physician.

Ultrasonic arteriography is used for routine screening of patients in stroke prone age groups and for the diagnosis and follow-up of patients with suspected carotid arterial disease. It is particularly valuable for studying patients with asymptomatic bruits and with non-localized symptoms. Clinicians are often reluctant to obtain an X-ray angiography in these patients because of the expense and hazards involved. However, X-ray angiography is still performed on the majority of patients prior to corrective surgery.

Figure 2. Position of ultrasonic transducer on the neck of a patient during an examination

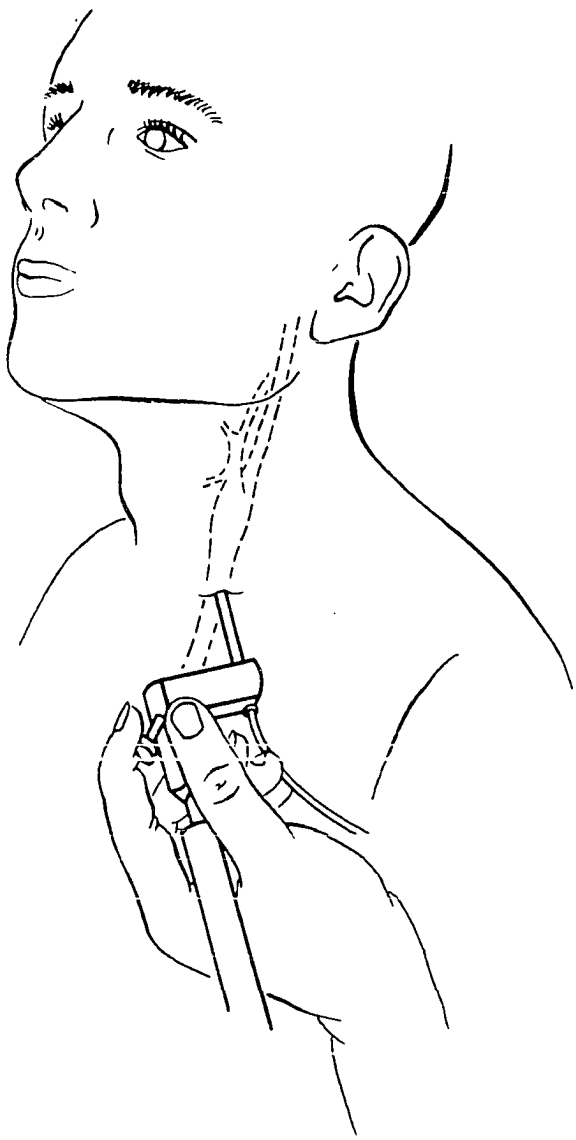

Due to inadequate resolution and lack of multiple views, ultrasonic images are reportedly misinterpreted in approximately 15% of the cases. This dissertation describes a microcomputer-aided pulsed-Doppler ultrasonic arteriograph which simultaneously produces two orthogonal views of the carotid arteries. The new instrument improves the diagnostic capabilities of Doppler ultrasound and should reduce the error caused by using a two-dimensional image to depict a three-dimensional artery. This approach is a significant new advance in instrumentation which promises to improve the selection of patients for the more hazardous and expensive radiographic examination.

LITERATURE REVIEW

This section will present an overview of the development of ultrasonic arteriography from the original ultrasonic motion detectors to the present day Doppler ultrasonic velocity meters and blood flow imagers.

Ultrasonic flow-velocity meters in use today have evolved over the past two decades. The original flowmeters were developed because of a pressing need for a means of non-invasively measuring blood flow in individual vessels.

Two approaches were taken in the search for a non-invasive blood flowmeter. The first approach was suggested by Kalmus (1954) and later applied by Franklin et al. (1959). Franklin's original flowmeter operated under the principle that the velocity of ultrasound is directly dependent on the velocity of the material in which it is traveling. His flowmeter consisted of a vessel cuff with two transducers, one pointing upstream and the other downstream. The crystals were on opposite sides of the vessel so that ultrasound transmitted by one crystal would be received by the other. Franklin pulsed the ultrasound first upstream and then downstream and by measuring the transit time between crystals, the average blood velocity was calculated.

The second approach, which is the most familiar, is based on the Doppler principle. Satomura (1959) was credited with the development of the first functional non-invasive Doppler flowmeter when he reported being able to detect blood flow transcutaneously. Shortly thereafter, Franklin et al. (1961) introduced a similar device for the detection of blood flow in animals. This device used a transducer with two crystals,

one continuously transmitting ultrasound and the other continuously receiving reflected ultrasound. When beamed into the tissue, a portion of the ultrasound is reflected from moving blood cells back toward the receiving crystal at a frequency which is shifted according to the basic Doppler equation. (See Background and Theory section for more detail.)

The reflected ultrasound wave strikes the receiving crystal which converts it to an oscillating voltage. The voltage is amplified and demodulated resulting in an audio signal whose Doppler shifted frequencies correspond to the flow velocities present. The person using this type of Doppler flowmeter can listen to the audio signal and with a trained ear, can discriminate between normal and disturbed blood flow.

Audible flow signals are usually converted by the flowmeter to a time dependent waveform, the magnitude of which approximates the mean velocity (frequency) of blood flow in the ensonated vessel.

There are two general methods of determining the mean Doppler frequency. The first method uses spectral analysis to calculate the magnitude of the frequency components which make up the Doppler spectrum. Integration of the spectrum yields the mean frequency. This method, although exact, is complex and cannot be accomplished in real-time. The other approach and the one in common use today was utilized by Franklin et al. (1961) in his early Doppler flowmeters. He applied zero-crossing detection to convert the complex Doppler signal to a series of pulses which were low-pass filtered to produce a voltage which is purported to represent the mean flow velocity. McLeod (1974) reports that instead of representing the mean velocity, zero-crossing detectors actually produce a voltage

that is proportional to the root-mean-square velocity. Other investigators have found that this can lead to an over-estimation of the mean flow velocity by up to 20 percent depending on such factors as signal amplitude, noise, and width of the power frequency spectrum (Reneman and Spencer 1974, and Baker et al. 1974). Even with this inaccuracy, zero-crossing detection is in wide use since it is an inexpensive yet simple method of producing a voltage which approaches the mean velocity.

One of the main limitations of the original Doppler flowmeters was their inability to discriminate between flow toward or away from the transducer. This was a major limitation because veins and arteries often lie adjacent to one another with blood flowing in opposite directions. When the vessels were both ensonated, the Doppler signal would contain composite arterial and venous flow signals making it difficult to separate and locate vessels.

Two methods were introduced to separate forward and reverse blood flow signals. In 1967, McLeod applied a technique used in radio communication called quadrature-phase detection to separate the Doppler shifted sidebands from the fundamental frequency. After detection, the phase separated forward and reverse Doppler signals are output to stereo headphones or zero-crossing detectors. (See Background and Theory section for more details.)

The other method of separating forward and reverse flow was developed by Nippa et al. in 1975. They applied a technique used in radio communication referred to as phase rotation, or outphasing, to separate the Doppler sidebands. Outphasing produces two independent

audio flow channels, one for forward flow and one for reverse flow. Nippa's innovative approach is very effective and is used in many functional Doppler flowmeters. Unfortunately, when compared with quadrature-phase detection circuits, outphasing circuits are more complex and thus more difficult to build and adjust.

Most commercial Doppler ultrasonic flowmeters available use quadrature-phase detection and zero-crossing detectors to produce two channels of average flow output. These instruments are used routinely in vascular clinics for semi-quantitative blood flow measurements at various locations along the course of the peripheral vessels. They can also be used to audibly analyze blood flow in the carotid and vertebral arteries.

The Doppler flowmeters discussed so far have been continuous-wave units which continuously transmit and receive ultrasound. With these instruments, the detected flow signal contains combined reflections from all vessels within the flowmeter's 4-10 cm range which may result in interfering flow signals. Therefore, in an effort to measure flow within a smaller tissue volume, Peronneau and Leger (1969) developed the range-gated or pulsed-Doppler flowmeter. With this type of flowmeter, a single piezoelectric crystal acts as both the transmitter and receiver. First, a short burst of ultrasound is transmitted into the tissue and after a calculated time delay the reflected ultrasound is sampled. The sample time measured in tenths of microseconds corresponds to a sample length of only 1-2 mm. In a classic paper, Baker (1970) outlines the theory and circuit design of pulsed-Doppler flowmeters along with discussions of ways to reconstruct velocity profiles using a single variable-depth sample gate.

In 1976, Keller et al. reported using a pulsed-Doppler ultrasonic flowmeter with 14 sample gates to reconstruct velocity profiles from flow measurements in the common carotid artery of patients with vessel obstructions.

From the basic continuous-wave and pulsed-Doppler ultrasonic flowmeters came the Doppler imaging systems. Two parallel paths have been followed, each with their strong and weak points. One group utilized continous-wave Doppler ultrasound to generate images of arteries and the other group utilized pulsed-Doppler ultrasound for imaging.

Reid and Spencer (1972) developed a continuous-wave Doppler imaging system for assessing patients with suspected carotid occlusive disease. Their instrument consisted of a continuous-wave Doppler ultrasonic flowmeter, transducer positioning arm and storage oscilloscope. By moving the transducer back and forth across a patient's neck over the carotid artery, flow points are displayed on the oscilloscope. As the exam progresses, the dots accumulate to form an image of the carotid artery. The image produced resembles a lateral projection of the vessel onto a two-dimensional plane. Since flow is detected with continuous-wave Doppler ultrasound, the instrument is not depth selective. Thus, if two vessels were in line with the sound beam, the flowmeter could not separate and display the vessels individually. This happens frequently enough with the internal and external carotids that it could conceivably cause a major diagnostic problem. Even with this problem, Spencer et al. (1977) and White and Curry (1978) report evaluating continuous wave imaging systems

in vascular clinics. They indicate that they could achieve 90% accuracy when detecting severe (> 50% diameter reduction) stenoses.

In 1971, a group at the University of Washington School of Medicine developed a pulsed-Doppler ultrasonic arteriograph which could non-invasively produce images of the carotid arteries of patients with suspected occlusive disease (Hokanson et al. 1971, Mozersky et al. 1971). Their instrument utilized six range gates to sequentially sample the Doppler signal reflected from six points across the vessel lumen. This depth selectively was used to produce transverse cross-sectional vessel images by moving the transducer in a direction perpendicular to the vessel axis while varying the gate range. By reconfiguring the transducer holder and repositioning the transducer arm, a longitudinal or plane image of the vessel could be produced. Hokanson continued to develop the pulsed-Doppler ultrasonic arteriograph and after some very promising clinical trials, he turned to commercial production.

In a clinical trial at Southern Illinois University School of Medicine, Russell et al. (1979) report using a Hokanson ultrasonic arteriograph to produce longitudinal images of the carotid arteries of 452 patients with suspected occlusive disease. At the discretion of the physician, X-ray angiography was performed on 107 of these patients. Comparisons were made between X-ray and UA images in 182 internal carotid arteries. Diameter stenoses estimated from the UA and X-ray images reportedly agreed within ±20 percent in 81% of the studies. If a greater than 40 percent area reduction is considered positive, the UA had a sensitivity of 88 percent and a specificity of 90 percent. However, the ultrasonic images were

incorrectly interpreted in 10 - 15 percent of the cases. In approximately 10 percent of the patients studied, localized calcium in the arterial walls prevented the penetration of ultrasound resulting in a blank region in the vessel image. Calcium was occasionally misinterpreted as an occlusion; however, calcified regions usually encompass only a small section of the image and would be diagnosed as a patent vessel with wall calcium if a normal lumen was imaged distal to the blank region. Russell et al. found that transverse cross-sectional views of the lumen at specific points along the carotid artery were not easy to obtain with the instrument since the transducer and positioning arm have to be reconfigured and reaimed. This maneuver results in a loss of spatial orientation so the examiner does not know the exact vessel location at which the transverse sectional image was made. An incorrectly located transverse sectional image is misleading and of questionable diagnostic value.

Other investigators have worked to improve arterial images produced by ultrasonic arteriography. Voss et al. 1977 reduced the image distortion of a pulsed-Doppler arteriograph by using a microcomputer to draw the vessel in its true plane. The microcomputer calculated the depth of the vessel relative to a fixed reference from transducer arm angles and the sample volume depth. Voss reports storing the two dimensional image in computer memory as it is produced during an examination. This is one of the first reports of a microcomputer being interfaced to an ultrasonic arteriograph.

The project described in this dissertation utilizes a pulsed-Doppler ultrasonic arteriograph and microcomputer to produce images of the carotid

arteries in orthogonal planes using three dimensional spatial information. This is an original idea which to this investigator's knowledge has not been attempted before.

BACKGROUND AND THEORY

A pulsed-Doppler ultrasonic arteriograph (UA) manufactured by D.E. Hokanson, Inc. was purchased in 1976 by Southern Illinois University School of Medicine for diagnosing patients with suspected carotid artery occlusive disease. Since that time, over 400 patients have undergone ultrasonic arteriography in the SIU vascular laboratory. If occlusive disease was found, the percent diameter stenosis was estimated from the ultrasonic images and when available compared to X-ray images of the same vessels. In 81 percent of the cases, diameter reduction estimates agreed within ±20 percent and were considered positive correlations. False positive and false negative ultrasonic diagnoses were made in 10-15 percent of the cases. Because of the 20 percent variance and the other diagnostic errors, ultrasonic arteriography has not been sufficiently accurate to preclude X-ray angiography prior to corrective surgery. However, if the diagnostic accuracy of ultrasound could be improved with better imaging, many patients may not have to undergo this expensive and somewhat traumatic X-ray procedure.

The following sections describe the potentials and limitations of ultrasonic arteriography along with an analysis of the operation of the Hokanson pulsed-Doppler flow detector used in this project.

The sequence of events leading to the detection of blood flow is initiated by short, repetitive, 8-cycle voltage bursts being gated from the 5 MHz oscillator to the piezoelectric crystal of the ultrasonic transducer (see Figure 3). This energy causes the crystal to vibrate at its fundamental frequency of 5 MHz for approximately 1.6 μsec. These

mechanical vibrations are transmitted as sound waves (i.e. pressure waves) into tissue through an aqueous coupling gel. The sound waves, in the ultrasonic range, are conducted through the tissue away from the transducer at an average velocity of 1560 m/sec. A portion of the ultrasonic pulse is reflected at interfaces of tissues with different accoustical impedances. (Where acoustical impedance is the product of the tissue density and the velocity of sound in the tissue.) If the ultrasound is reflected from a stationary acoustical interface, the reflected frequency will remain unchanged. However, if the interface is moving, as is the case with red blood cells and vessel walls, the reflected frequency will be shifted according to the familiar Doppler equation:

$$f_d = f_o + \frac{2\, v f_o \cos\theta}{c}$$

where:

f_d = Doppler shifted frequency of the reflected ultrasound

f_o = Fundamental transmitted frequency

v = Velocity of moving interface (e.g. blood cells)

θ = Theta, angle between incident sound beam and velocity vector of interface

c = Velocity of ultrasound in tissue

The Doppler frequency shift, Δf, is equal to:

$\Delta f = | f_o - f_d |$, frequency change caused by moving interface

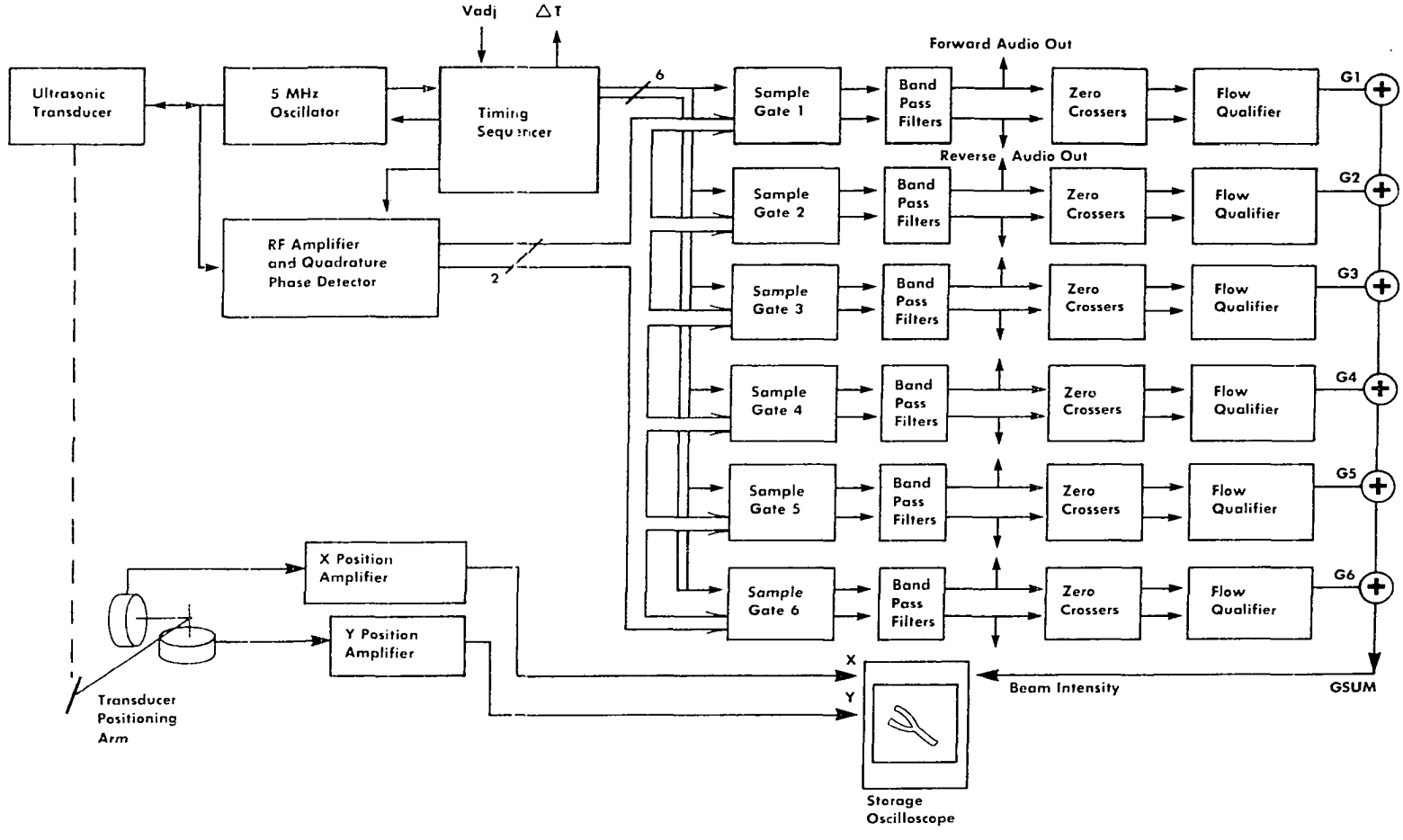

Figure 3a. Block diagram of Hokanson ultrasonic arteriograph

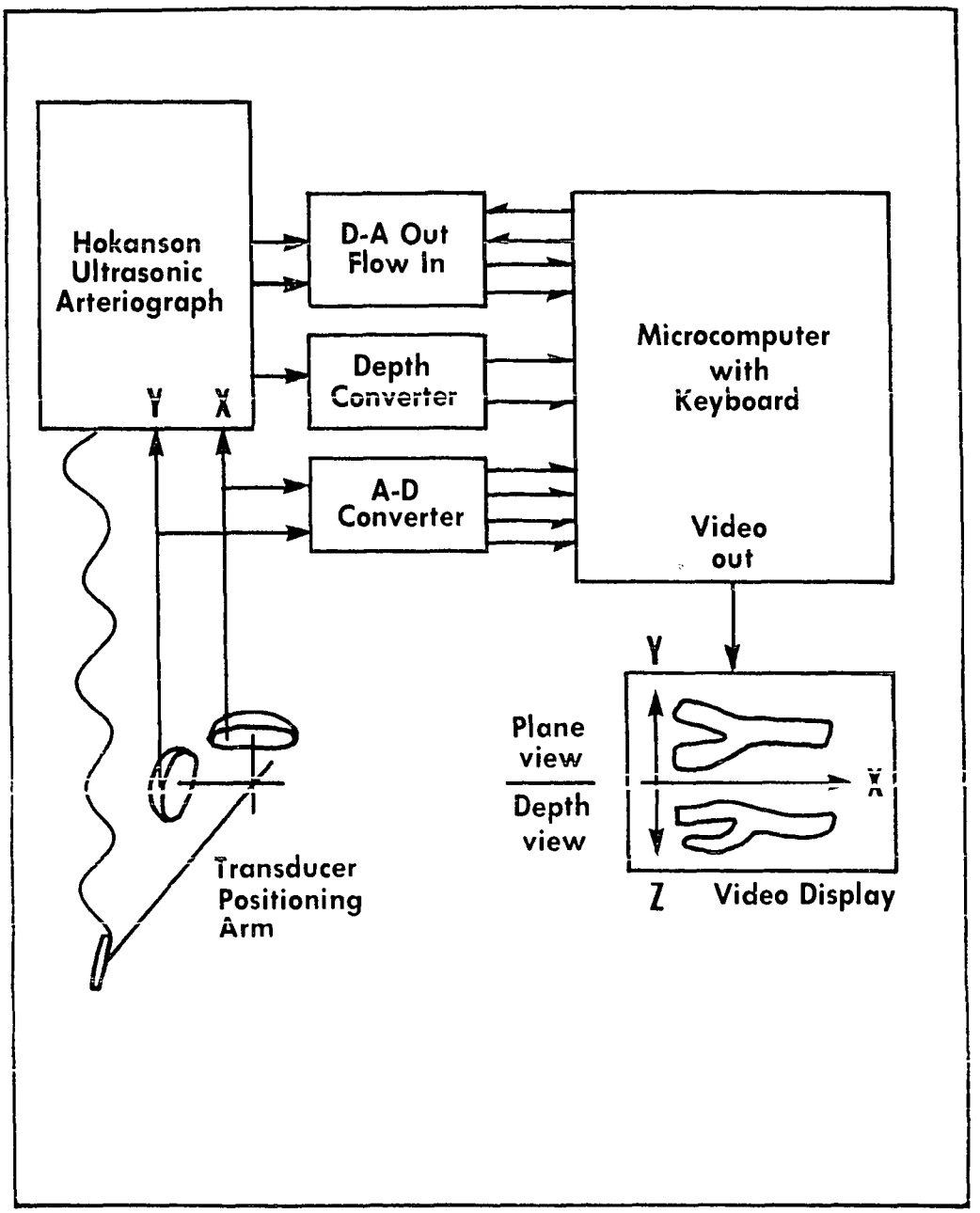

Figure 3b. Block diagram of new microcomputer-aided ultrasonic arteriograph.

Figure 4. Timing diagram for the Hokanson ultrasonic arteriograph

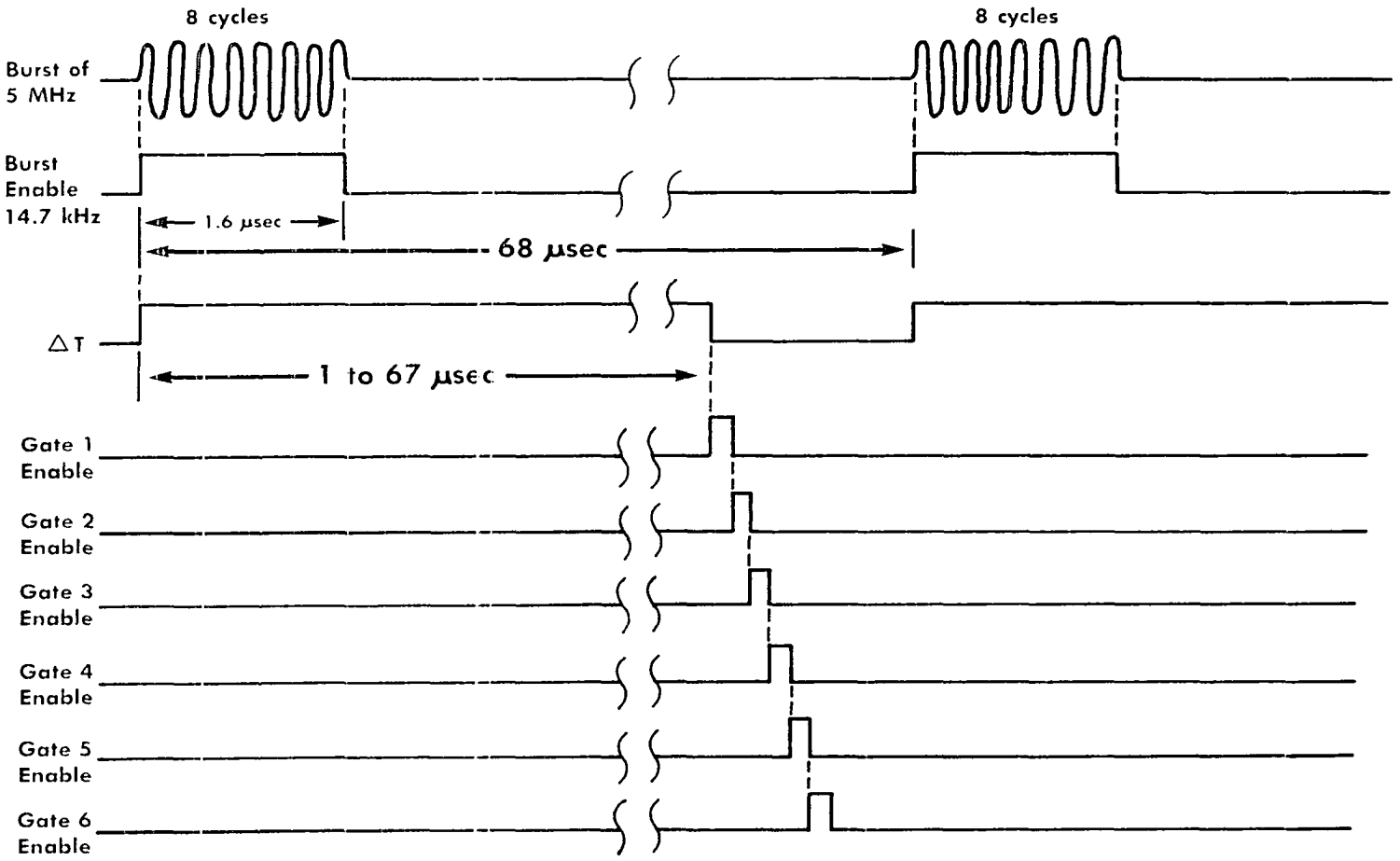
8 cycles
8 cycles
Burst of
5 MHz
Burst
Enable
14.7 kHz
1.6 μsec
68 μsec
ΔT
1 to 67 μsec
Gate 1
Enable
Gate 2
Enable
Gate 3
Enable
Gate 4
Enable
Gate 5
Enable
Gate 6
Enable

During the time between bursts, the same crystal acts as a receiver to convert reflected sound waves back into oscillating voltages. Baker (1970) estimates that 5 MHz ultrasound is attenuated approximately 20 dB/cm of tissue depth and another 20-40 dB is lost due to Raleigh type scattering by the blood cells. In addition to these losses, 20-40 dB of ultrasonic energy is lost due to the poor impedance match between the crystal and the tissue. These losses accumulate so the intensity of the detected reflections may be decreased by 60 to 120 dB from that transmitted. These losses are partially regained by the RF amplifier of the ultrasonic arteriograph which is block diagrammed in Figure 3. The gain of the RF amplifier varies with time (range gain) so attenuated reflections from deep tissues are amplified more than reflections from shallow tissues.

The voltage output from the RF amplifier is demodulated by a quadrature-phase detector developed initially for this application by McLeod (1967). The detector removes frequencies produced by reflections from stationary interfaces and separates by phase the Doppler sideband frequencies produced by moving interfaces. The phase relationship between the outputs of the demodulator determines whether detected flow is advancing or receding.

Signals output from the demodulator circuit are sequentially sampled by six sample gates at 14.7 kHz, a rate equal to the pulse repetition frequency (PRF) of the 5 MHz ultrasonic bursts (see Figure 4). According to the sampling theorem this limits the maximum detectable Doppler frequency to one-half the PRF or 7.35 kHz. For the ultrasonic arteriograph,

a 7.35 kHz Doppler frequency corresponds to a flow velocity of 160 cm/sec when the probe angle is 45^{o}. This is the maximum velocity that can be present in the vessel if aliasing errors are to be prevented. In practice, very few red blood cells attain a velocity of 160 cm/sec in the carotid arteries. A PRF of 14.7 kHz leaves approximately 67 μsec between bursts for the ultrasound to travel into the tissue and back. Since the velocity of ultrasound in tissue is a finite 1.5×10^{6} mm/sec, ultrasound can travel to and from a tissue depth of 43 mm before the next burst is sent out. Fortunately, a 43 mm depth is sufficient for most carotid artery examinations.

The output from each sample gate is filtered to pass Doppler frequencies between 8 kHz and 230 Hz. The 8 kHz upper cutoff frequency is required to remove the 14.7 kHz pulse repetition frequency component of the Doppler signal, while the 230 Hz cutoff frequency removes low frequency motion artifacts caused by pulsating vessel walls and transducer motion. Each filtered signal is input to a zero-crossing detector (ZCD) which converts the Doppler signal to a series of pulses. These pulses are lowpass filtered to produce a voltage whose amplitude approximates the desired mean frequency (velocity) of the Doppler signal. (McLeod (1974) reports that the output from the ZCD is actually the root-mean-square Doppler frequency rather than the mean frequency.) In each channel, the outputs from both zero-crossing detectors are compared to see which pulse leads in time. A leading pulse edge in one channel indicates flow is toward the transducer while a leading pulse edge in the other channel indicates flow is away from the transducer.

After the operator selects either forward or reverse flow to be imaged, the appropriate signal is input to a flow qualifier. When flow duration is maintained for 20 ms, the flow qualifier outputs short +5 volt pulses. (The flow qualifier is needed to prevent short, random noise bursts from erroneously indicating flow.) In the Hokanson UA, the output voltage pulses from each of the six flow qualifiers are asynchronously ORed and fed to the intensity input of a bistable storage oscilloscope. When flow is detected within a gate interval, a pulse is generated producing a dot on the screen of the cathode ray tube (CRT). Dot location on the CRT is determined by a positioning arm which holds the ultrasonic transducer. The positioning arm allows three directions of transducer motion, two of which are mechanically coupled to precision linear potentiometers. These two potentiometers define the x and y transducer motion in a plane parallel to the face of the transducer. The third direction of motion along the long axis of the transducer is not detected causing minor spacial distortion of the vessel image.

The ultrasonic pulse length, beam width and gate sample time determine the size of the sample volume. In the Hokanson UA, the range and spacing between six sample gates are adjusted by the examiner so the sample volumes lie within the lumen of the vessel.

The theoretical lateral resolution of the vessel image in the x and y directions is a function of the beam width. Since the beam is transmitted from a circular crystal, it assumes a cylindrical shape whose radius equals that of the crystal for a distance X_0 in a region called

the near field or Fresnel zone. The length X_o of the near field can be calculated from the equation:

$$X_o = \frac{r^2}{\lambda} = \frac{r^2 f}{c}$$

where: r = radius of the transducer crystal

λ = wavelength of the ultrasound

c = velocity of ultrasound in tissue

f = frequency of ultrasound

since: r = 19 mm

$f = 5 \times 10^6$ Hz

$c = 1.56 \times 10^6$ mm/sec

then: X_o = 11.6 mm, (near field length)

After the near field, the beam begins to diverge in the far field or Fraunhofer zone which can be represented as a cone with its apex at the center of the crystal. The cone diverges with the half angle ϕ, where ϕ is defined by the equation:

$$\tan \phi = \frac{\lambda}{r} = \frac{c}{fr}$$

When the same values for the variables c, f and r are used, the half-angle ϕ equals

$$\phi = \tan^{-1} (.16) = 9.3^o$$

With this angle, the beam radius (r_1) at the average depth of an internal carotid (z_1), can be calculated from the equation for the radius of the base of a cone:

$$r_1 = z_1 \tan \phi$$

if: $\phi = 9.3^{o}$

$z_1 = 15$ mm

then: $r_1 = 15 \tan (9.3)$

$r_1 = 2.4$ mm (beam radius at 15 mm depth)

Lateral resolution is better than would be indicated from the beam radius since the energy of the beam is not constant across its cross-section. Lloyd (1967) reports the beam intensity has a maximum in the center and decreases toward the periphery due to the tear drop shape of the pulse. This accounts for the lower intensity of the reflections from the peripheral regions of the beam that are practically eliminated by the noise limiting circuits of the flowmeter. This investigator has determined the lateral resolution of the UA by measuring ultrasonic arterial images and comparing these measurements with X-ray images of the same vessel. For a carotid artery 2 cm deep, ultrasonic lateral resolution is on the order of 1 mm. This resolution measurement is supported by the UA manufacturer, D.E. Hokanson, Inc.

The length of the sample volume defines the ultrasonic depth resolution and is determined by the time the sample gate is open (Δt) and the length of the emitted pulse (t_p). Since the ultrasound wave front

must travel across the sample volume and back again, the gate time is actually twice the sample volume length. Thus, when the gate time of the UA is set at 1.4 μsec, the equation to calculate the gate contribution to the sample volume length is

$$l_g = \frac{c\Delta t}{2}$$

if: $c = 1.6$ mm/μsec (velocity of ultrasound)

$\Delta t = 1.4$ μsec

then: $l_g = 1.1$ mm

The additional effect of the pulse length is found by considering a finite pulse length t_p with a gate time that approaches zero. In this case the wave front of the back-scattered ultrasound at any one point along the beam axis will contain information from a sample length (l_p) of $ct_p/2$. Where $t_p/2$ is the time it takes for the back-scattered ultrasound to travel from the leading edge of the incident pulse to the trailing edge (Morris et al. 1973). The equation for the pulse length contribution to the sample volume length is

$$l_p = \frac{ct_p}{2}$$

if: $c = 1.6$ mm/μsec

$t_p = 1.2$ μsec

then: $l_p = 0.8$ mm

By combining the equations, the sample volume length (l_{sv}) equals the sum of the two components:

$$l_{sv} = l_g + l_p = 1.9 \text{ mm}$$

Flow detection by the individual sample gates is indicated by six light emitting diodes (LEDs) on the front of the UA. During a patient examination, the examiner moves the transducer back and forth across the patient's neck while adjusting the depth range so the sample gates lie within the vessel lumen. The gate times are normally set for minimum spacing which yields a theoretical total sample length of 1.9 x 6 = 11.4 mm. When the transducer is inclined 45^{o} relative to the vessel axis, the distance across an 8 mm vessel is 8 /cos 45^{o} = 11.3 mm which allows all sample gates to lie within the lumen of the vessel.

When flow is detected by any of the six sample gates, the UA places a dot at the appropriate place on the CRT screen. With repeated passings of the transducer, the dots coalesce to form an image of the carotid artery. An example of an ultrasonic examination of a patient with a diseased left internal carotid along with X-ray pictures of the same vessel are shown in Figure 5. Ultrasonically the patient was diagnosed as having a 40 - 60 percent diameter reduction of the left internal carotid artery which was confirmed with X-ray examination.

Figure 6 shows the ultrasonic image of the same patient's right carotid which was diagnosed as normal. However, subsequent X-ray examination detected a 60 percent diameter reduction of the right internal carotid artery. This error was attributed to the stenosis not being visible from the direction of the ultrasound beam.

Figure 5a. Image of a left carotid bifurcation produced by the ultrasonic arteriograph showing a 40 - 60 percent diameter reduction of the internal carotid artery.

Figure 5b. Lateral X-ray image of the same left carotid bifurcation confirming the diagnosis of the ultrasonic image.

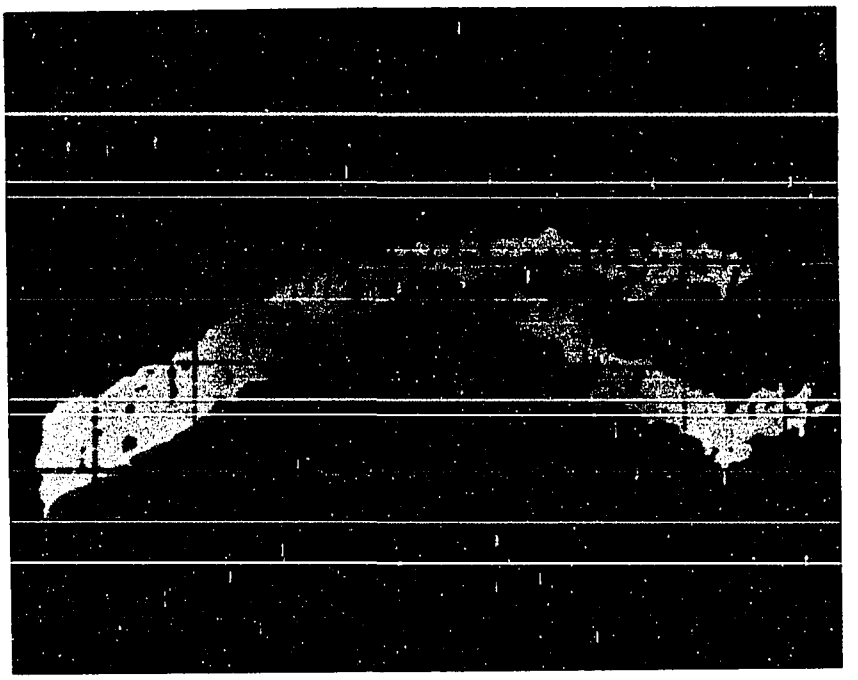

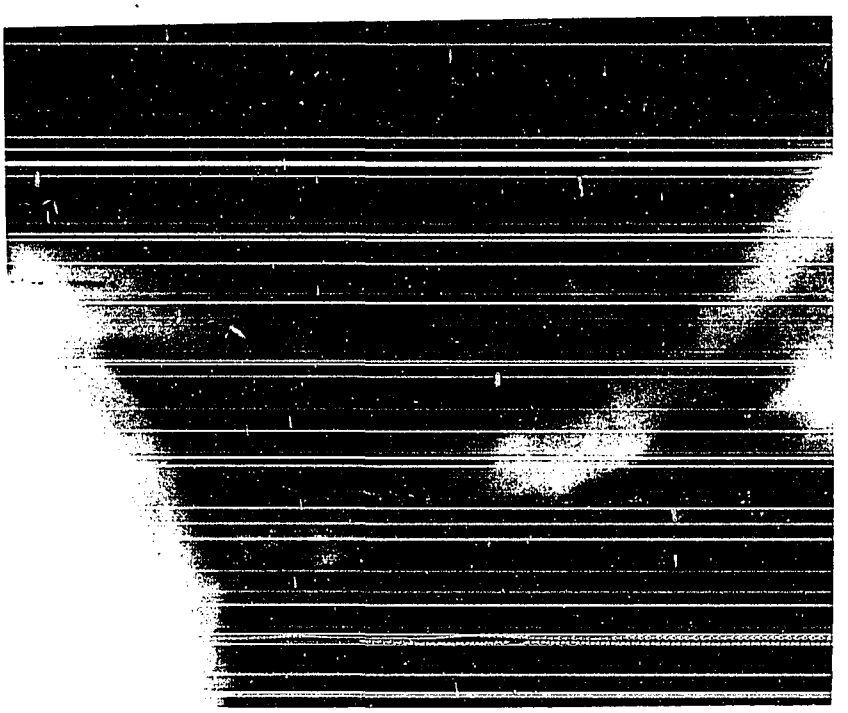

Figure 6a. Image of a right carotid bifurcation produced by the ultrasonic arteriograph showing an apparent normal internal carotid artery which after X-ray examination (see below) was diagnosed as having a severe occlusion. This case shows the need for better ultrasonic imaging.

Figure 6b. Lateral X-ray image of the same right carotid bifurcation showing a 60% diameter reduction of the right internal carotid artery.

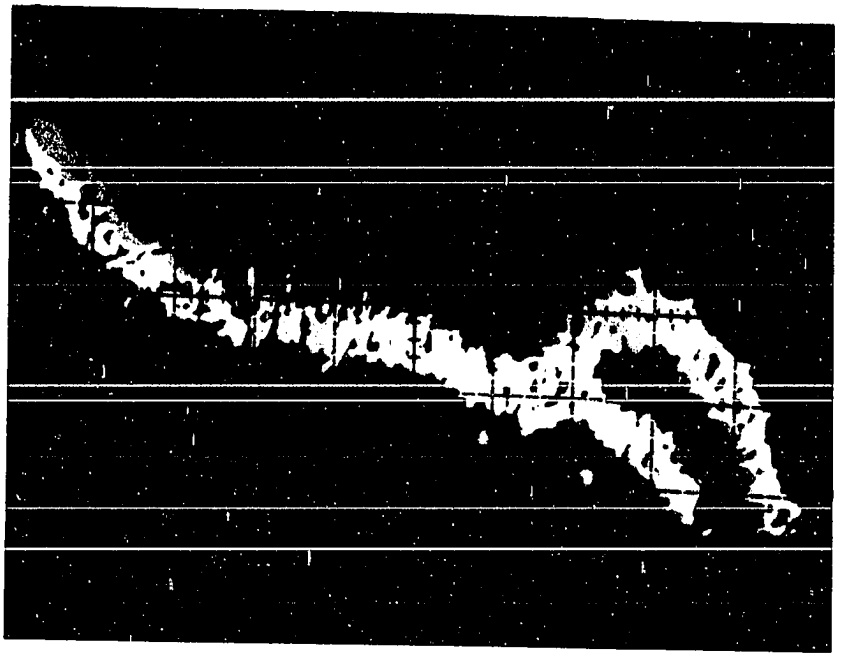

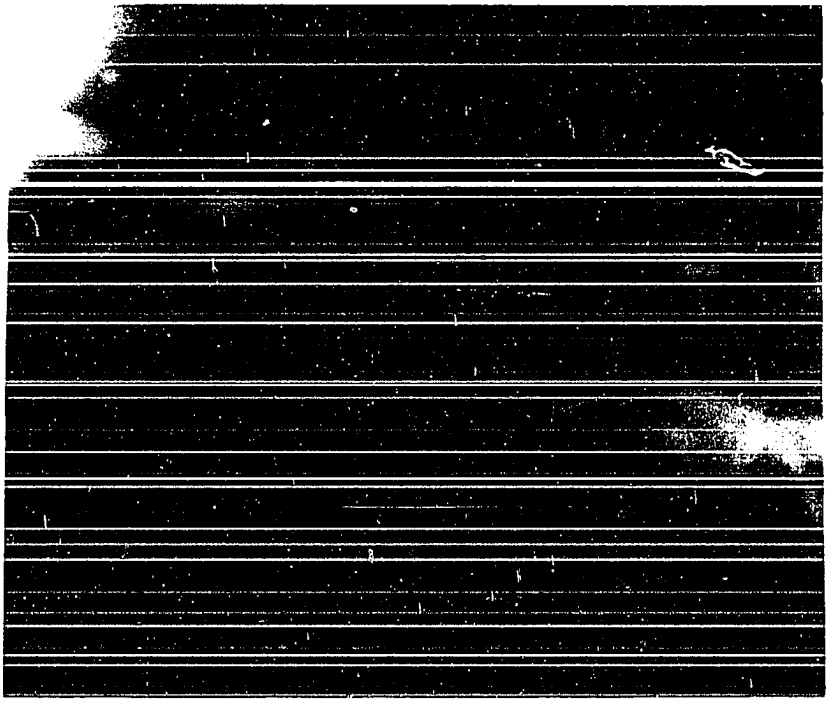

The need for better arterial images was realized after discussions with several vascular surgeons who routinely used the Hokanson UA. After personally observing and participating in the ultrasonic examination of a number of patients and volunteers, the imaging problem began to surface. Resolution on the oscilloscope image was good enough to estimate the percent diameter stenosis within ±20 percent in 81 percent of the vessels imaged. This ultrasonic accuracy was sufficient for the routine screening of patients but was not good enough to eliminate the need for X-ray examination prior to corrective surgery. It was felt that the main reason for the variance in estimated diameter was due to the physician using a two-dimensional image to estimate the size of a three-dimensional, asymmetrical stenosis. This estimation method produces errors. The UA is designed so an image dot will be placed on the screen if one or more sample gates detects flow. Therefore, if only one gate detects flow, the vessel appears patent at that location. For example, even if the far half of a cylindrical vessel was occluded, the vessel would appear perfectly normal in the UA image. This problem could be corrected if an additional view of the vessel was available which imaged flow from the side of the vessel.

Another imaging problem presents itself when the examiner encounters a vessel that changes in course until the vessel is perpendicular to the transducer beam. This orientation results in no Doppler shift with a subsequent blank region on the vessel image. Since the ultrasonic image does not indicate the depth of the vessel, the physician may incorrectly interpret the blank region as a complete vessel occlusion.

Therefore, a vessel image which also displays the depth of the vessel as it courses through the neck would be a valuable diagnostic aid.

The Hokanson UA uses pulsed Doppler ultrasound and six sequential range gates to sample flow at known tissue depths. Depth coordinates of the sample volumes are available within the UA but are not used to produce vessel images. Therefore, it was hypothesized that X, Y transducer position coordinates and depth coordinates of the sample volumes could be used to produce "three-dimensional" images of the carotid arteries. The problem of how to display a vessel in three dimensions posed an immediate problem since only flat two-dimensional screens are available. A linear perspective image would make the vessel appear three-dimensional but was considered to be too difficult to implement. Moreover, a perspective image would result in hidden surfaces. Since the idea was to display more vessel surfaces, a perspective image was deemed unacceptable. Because most physicians are familiar with X-ray images of the carotid arteries, it was decided that the best way to show a three dimensional vessel would be to use two views similar to lateral (plane) and anterior-posterior (depth) X-ray views. The physician could use these two views, which contain three-dimensional spatial information about a vessel, to more accurately determine the size of a three-dimensional stenosis. Moreover, the depth view could be used to map the course of a vessel relative to the skin. This would explain blank regions on the vessel image caused by a vessel coursing out of the 4 cm range of the UA or by a vessel turning perpendicular to the sound beam thereby eliminating the Doppler signal.

An ultrasonic image is actually a projection of the vessel onto a plane. The ultrasonic lateral view corresponds to a projection of the vessel on a plane approximated by the skin of the neck and defined by the x, y motion of the transducer where the x direction is along the major axis of the artery. In contrast, the ultrasonic depth view is a projection of the vessel onto a plane perpendicular to the x, y plane of the neck where the image is produced by the x motion of the transducer along the skin and the range (z) of the sample volumes perpendicular to the x, y plane.

During a patient examination the X, Y transducer coordinates and the depth of the sample volume are continually being measured by the ultrasonic arteriograph. This spatial information can be utilized along with flow data to draw two views of the carotid artery at the same time. With this type of display, the time required for the ultrasonic examination would not be increased and the transducer would have the same orientation since neither the patient's position or the transducer approach would change.

The storage oscilloscope contained within the ultrasonic arteriograph was too small to display both plane and depth views of the artery so a new approach was needed. It was hypothesized that a microcomputer could be used to digitize flow and position signals from the UA and produce arterial images on a video screen. In addition, microcomputer programming would promote system flexibility and allow easy control of signal inputs and vessel images.

The next section describes the new microcomputer-aided ultrasonic arteriograph developed to produce images of the carotid arteries with three dimensions on a video screen. This is a new and innovative approach which promises to improve the diagnostic capabilities of ultrasonic arteriography.

MATERIALS AND METHODS

The objective of this project was to improve the diagnostic capabilities of the Hokanson pulsed-Doppler ultrasonic arteriography (UA) by using flow and position information to generate arterial images with three dimensions. Since the Hokanson UA uses pulsed-Doppler ultrasound, the depth of the ultrasonic sample volume is determined along with its x, y position. This is sufficient position information to identify the three-dimensional coordinates of the ultrasonic sample volume. During an examination, these coordinates are digitized and input to an online microcomputer which simultaneously produces two orthogonal views of the artery on a video screen. One view is a plane projection which is similar to a lateral view obtained with X-rays while the other view is a depth projection which is similar to an anterior-posterior (A-P) X-ray view.

Materials

Twelve signal lines necessary for the production of arterial images were brought to a front panel connector on the UA for easy transfer to a microcomputer via interface boards. The signal lines from the UA are

X - A dc voltage corresponding to the x-position coordinate of the ultrasonic transducer.

Y - A dc voltage corresponding to the y-position coordinate of the ultrasonic transducer.

ΔT - A 14.7 kHz pulse-width modulated square wave whose width corresponds to the variable time between transmission of the ultrasound burst and the opening of the first sample gate. This signal determines the depth of the sample gates.

V_{adj} - The voltage adjust pin on the timer which generates ΔT. Applying 0 to +5 volts on this line causes the gate depth to vary from minimum to maximum.

GSUM - The binary sum of the outputs from the six flow gates. When this line is high, flow is detected by the UA; when low, flow is absent.

G6 - Binary indication of flow detection by gate 6

G5 - Binary indication of flow detection by gate 5

G4 - Binary indication of flow detection by gate 4

G3 - Binary indication of flow detection by gate 3

G2 - Binary indication of flow detection by gate 2

G1 - Binary indication of flow detection by gate 1

Gnd - Common UA circuit ground

A microcomputer was selected to input these 12 signals from the UA. The following list describes the criteria applied in the selection process:

1) The cost of the microcomputer must be within the $3500 equipment budget for this project. This was a reasonable upper limit on price because the Hokanson UA presently costs around $15,000.

2) The microcomputer must be capable of bit-mapped high resolution color graphics where each graphic dot corresponds to an addressable bit in computer memory. Color graphics capability would improve vessel identification.

3) A high-level language must be available to simplify software development.

4) Circuit board connectors must be provided for the addition of custom designed interface boards.

5) Extensive hardware and software documentations must be provided.

6) Floppy disk drives must be included for the storage and retrieval of programs and vessel images.

7) If budgetable, a printer would speed software development.

Based on these criteria, a 6502-based microcomputer manufactured by Apple Computer, Inc. of Cupertino, California was selected. The system consists of an Apple II microcomputer with integral keyboard, 48K of read/write memory, a BASIC interpreter, dual 5-inch floppy disk drives, a Centronics model P1 thermal printer and a 19-inch Sony model CKV-171, 19-inch color television receiver (see Figure 7). BASIC statements are available to plot points on a video screen in a 280 x 192 dot matrix. Each of the 53,760 possible display points are stored as individual bits in a block of computer memory for easy updating of the display. Multi-color high resolution graphics can be created by changing the dot color to white, red, blue, green, or black. This microcomputer system met or exceeded all of the above requirements.

SOFTWARE

A BASIC interpreter and machine language assembler were included with the Apple II microcomputer. BASIC is an easy to learn, high-level computer language which was designed for medium length, interactive programs. Since BASIC must interpret each line of the program while the program is running, execution speed is relatively slow. Fortunately, when speed is required, BASIC has a CALL statement which allows the calling of a faster machine language subroutine. Powerful POKE and PEEK statements are available to store or read a byte of data from memory. These statements, along with special high-resolution graphic commands make the BASIC language ideal for the control of interface boards and the generation of arterial images. The microcomputer has 49,152 words (48k) of 8-bit read/write memory into which must be loaded the disk operating system

Figure 7a. The microcomputer is shown connected to the ultrasonic arteriograph with the investigator at they keyboard.

Figure 7b. Apple microcomputer with keyboard is shown along with two floppy disk drives and video monitor with an arterial image previously stored on disk.

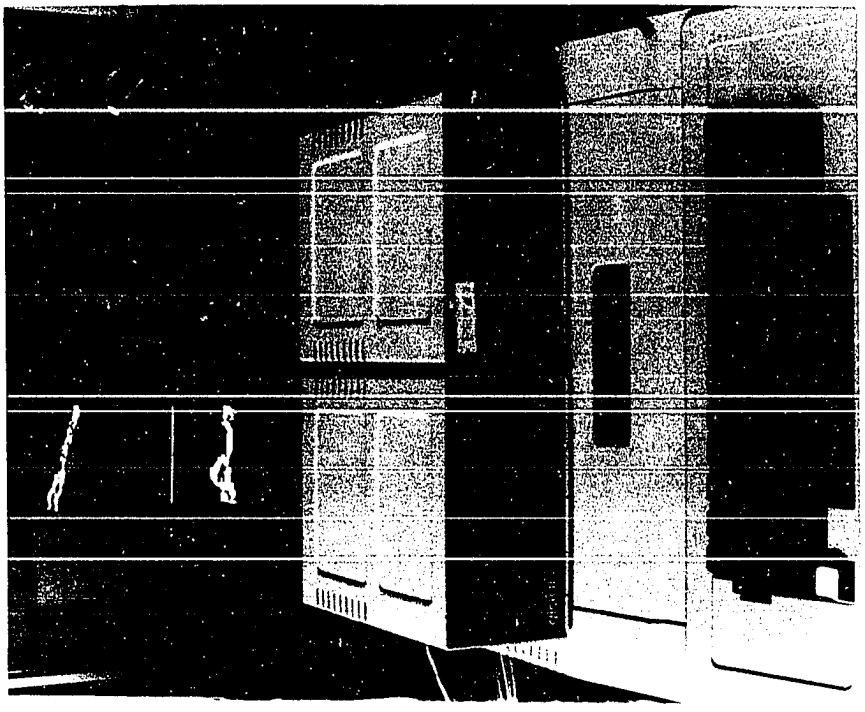

(10K), the BASIC program (1.7K), and the machine language subroutine (30 words). An additional 8K block memory is also reserved for the 53,760 dots which make up the image matrix.

BASIC programs were written to control microcomputer interface boards designed to digitize signals from the ultrasonic arteriograph for the generation of arterial images. Interfacing to the Apple II microcomputer is done through eight 50-pin card-edge connectors on the back of the microcomputer. Each connector provides all the power, address, data and control lines necessary for an interface board. Two of the eight connectors are used for printer and floppy disk controller boards manufactured by Apple Computer, Inc. Three of the remaining connectors are used for: a two-channel analog-to-digital converter board; a parallel input/output and digital-to-analog converter board; and an interface board which converts the pulse width of the ΔT square wave to a digital word. A complete description of the design and operation of the interface boards follows this section.

Analog-to-digital interface

A two-channel analog-to-digital (A-D) interface board was designed and built to digitize the X and Y transducer position voltages from the Hokanson UA. A photograph of the interface board is shown in Figure 8 and a circuit schematic in Figure 9.

The circuit consists of a precision voltage regulator which provides the required stable reference voltage for A-D conversion. Two input amplifiers with variable gain and offset amplify the transducer position voltages for the 0 to +10 volt range necessary for A-D conversion. Two

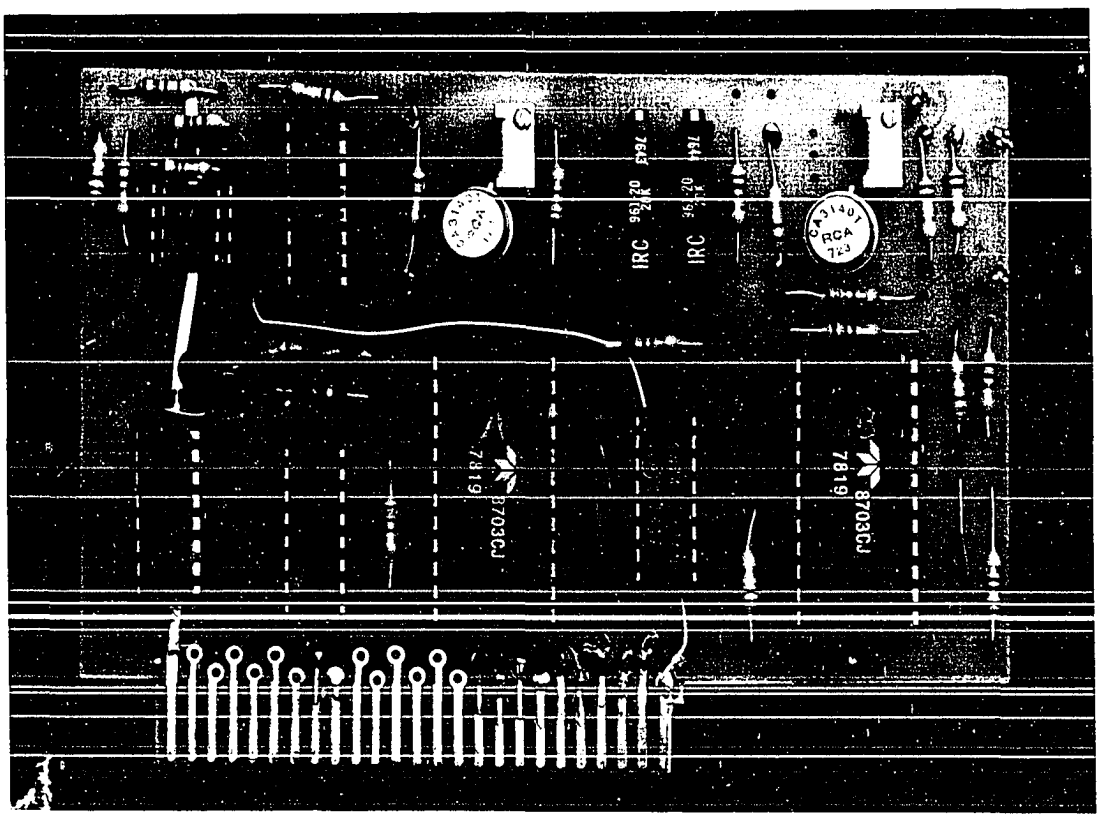

Figure 8. Photograph of analog-to-digital interface board used to digitize X and Y position voltages

Figure 9. Analog-tc-Digital interface circuit diagram showing two A-D converter channels.

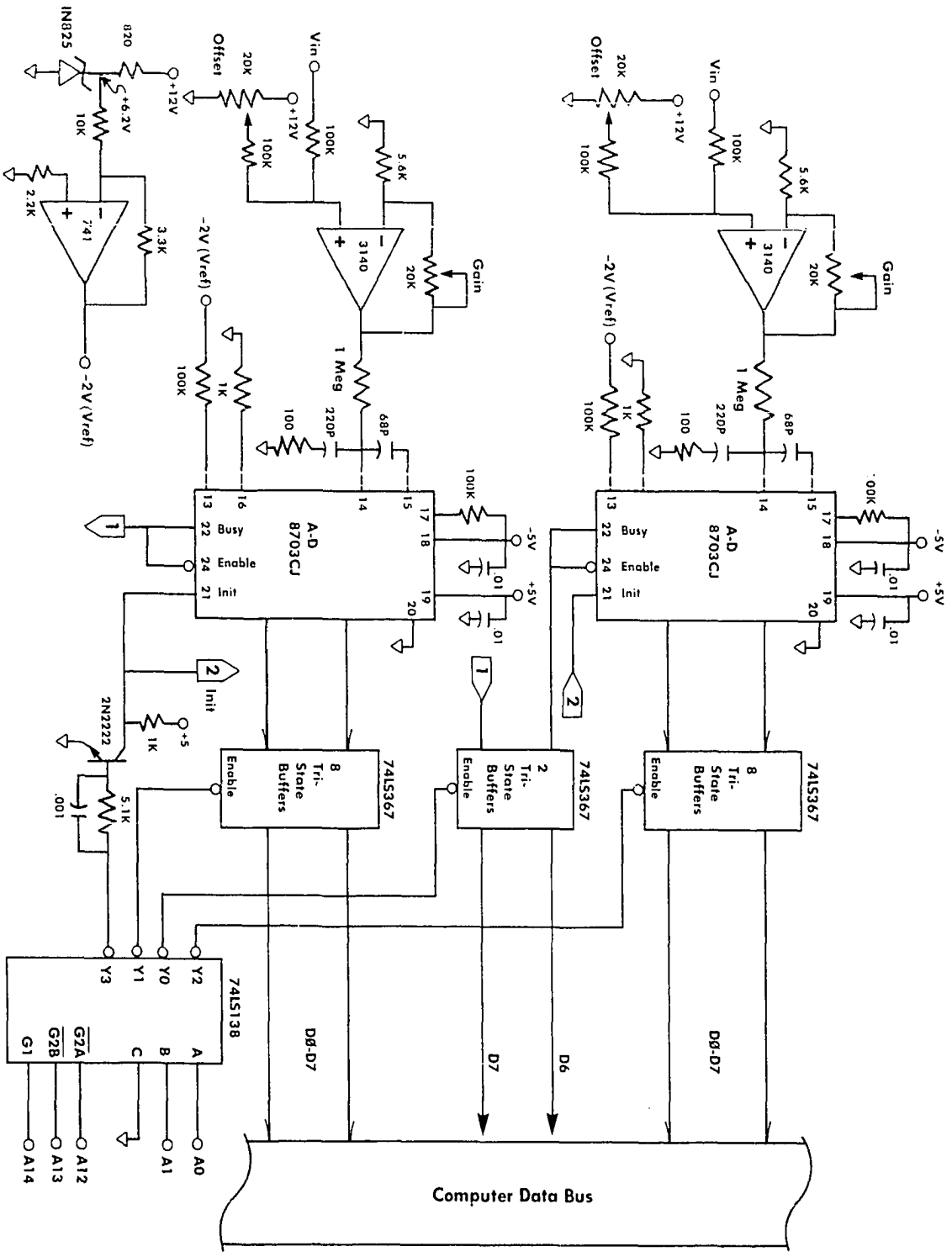
Offset
20K
+12V
100K
Vin
100K
5.6K
3140
20K
Gain
-2V (Vref)
100K
1K
1 Meg
100
220P
68P
.00K
-5V
+5V
.01
A-D
8703CJ
13
22
24
21
Busy
Enable
Init
15
17
18
19
20
1
2
74LS367
8
Tri-
State
Buffers
Enable
2
Tri-
State
Buffers
D0-D7
D7
D6
Computer Data Bus
74LS138
Y3
Y1
Y0
Y2
G1
G2B
G2A
C
B
A
A14
A13
A12
A1
A0
IN825
820
+6.2V
10K
2.2K
741
3.3K
-2V (Vref)
2N2222
1K
+5
5.1K
.001

Teledyne 8703CJ, 8-bit monolithic CMOS analog-to-digital converters were used because of their low cost ($12), high accuracy (<±½ LSB error), low power dissipation (<20 mW), and microprocessor compatibility (8-bits). Low-power Schottky (LS) TTL integrated circuits were selected for the address decoders and three-state buffers because of their fast switching speed and low power consumption.

The A-D interface board was designed with separate microcomputer addresses assigned to the A-D control, status and data lines. Thus, under program control, the address decoder can select one of the following: 1) initiate A-D conversion in both converters, 2) enable the three state buffers to load the conversion status onto the data bus, 3) enable the three-state buffers to load the X-converter data onto the data bus, or 4) enable the three-state buffers to load the Y-converter data onto the data bus.

To evaluate the interface board, the X and Y position voltages from the UA were connected to the A-D converter board with a 3-conductor, shielded cable. When the transducer was moved through its 10 cm x 13 cm range, the position voltages varied between ± 2.5 volts. Since the A-D converters require 0 to ±10 volts for full range conversion, the offset and gain of the input amplifiers had to be adjusted. A short BASIC program was written to control the A-D conversion and to produce transducer position dots on the video screen. The program was run and the dots were drawn to trace the path of the transducer. This test confirmed the operation of the A-D converters. The next step was to draw a plane arterial view on the video screen from X and Y position voltages recorded

on FM tape during an actual ultrasonic arteriography procedure. The detailed image that resulted proved that the A-D conversion was fast enough and that the graphics resolution was more than adequate for arterial imaging.

Parallel I/O and D-A interface

A combination 8-bit parallel input/output (I/O) and digital-to-analog (D-A) converter circuit board was designed and built to input flow data from the six gates of the UA and to control gate depth during a vessel search cycle (see Figure 10). A block diagram of the circuit is shown in Figure 11 and a circuit schematic in Figure 12.

The circuit contains two Rockwell R6522 versatile interface adapter (VIA) integrated circuits. These ICs each contain two interval timers, a serial-to-parallel/parallel-to-serial shift register, dual 8-bit parallel I/O ports and four control lines in a 40-pin package. In addition to the two VIAs, this circuit has two 8-bit, complementary current-output DAC-08 digital-to-analog converters manufactured by Precision Monolithics, Inc. The complementary current-outputs of the DACs drive the differential inputs of CA3140 op amps for conversion to a single-ended voltage output. A CA3140 op amp and a 1N825 reference diode generate a stable reference voltage for the D-A converters. The 8-bit outputs from Port A of each VIA can drive a D-A converter or simply function as a parallel I/O port if the D-A converters are removed from their sockets. An additional 74LS138 address decoder is used to decode the chip select address for each VIA.

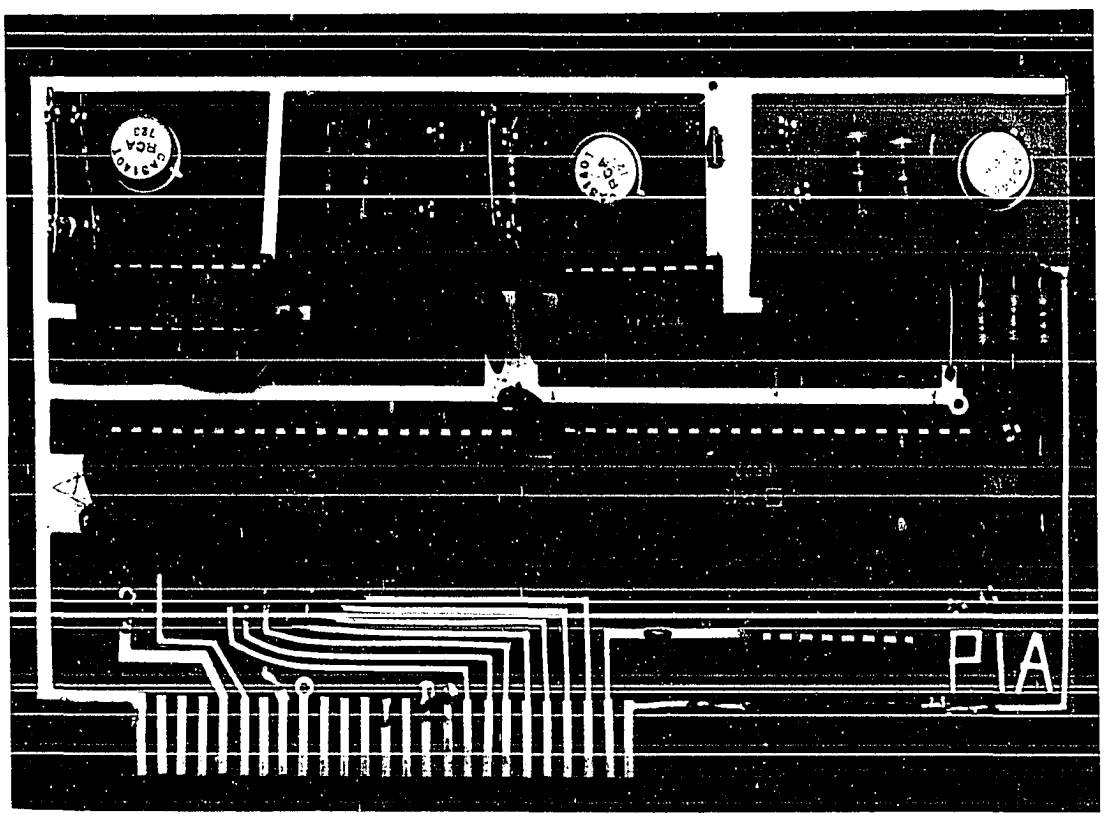

Figure 10. Photograph of parallel input/output interface board used to input flow data

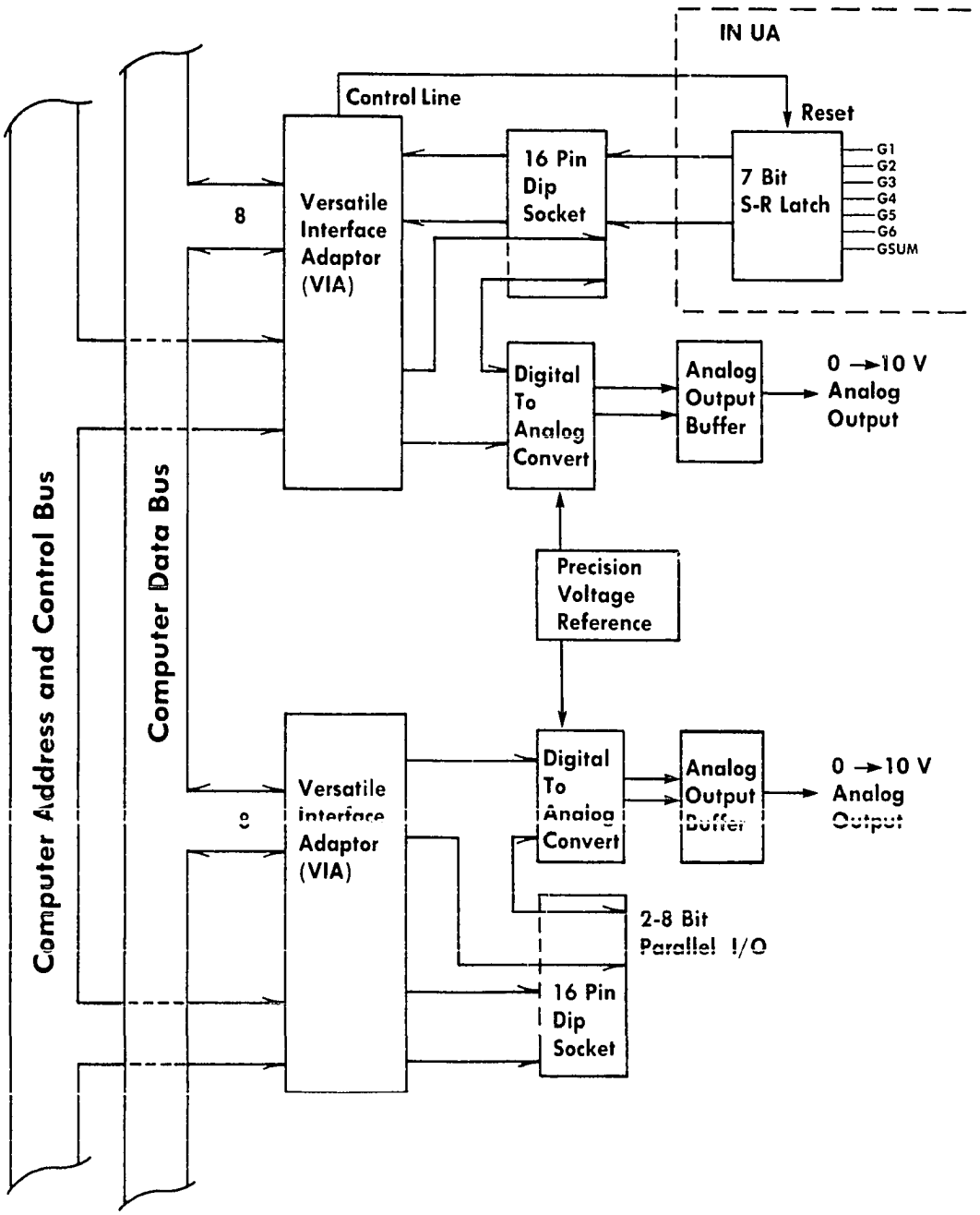

Figure 11. Block diagram of parallel input/output interface board.

Figure 12. Parallel input/output and digital-to-analog interface circuit schematic used to input flow data.

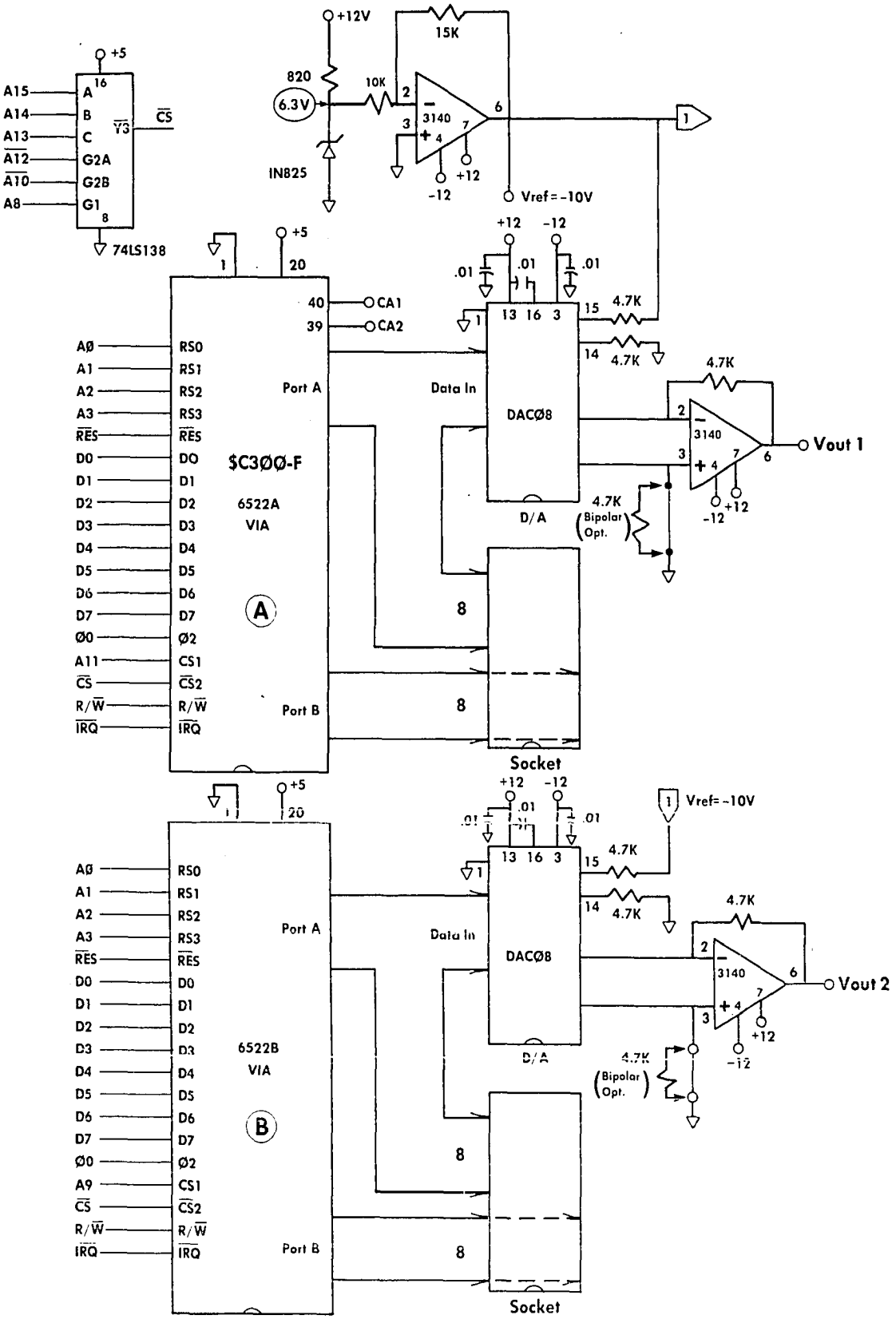
+12V
15K
820
6.3V
10K
IN825
3140
-12
+12
Vref=-10V
+5
A15
A14
A13
A12
A10
A8
74LS138
CS
Y3
$C3ØØ-F
6522A
VIA
Port A
Port B
CA1
CA2
RS0
RS1
RS2
RS3
RES
DO
D1
D2
D3
D4
D5
D6
D7
Ø2
CS1
CS2
R/W
IRQ
A0
A1
A2
A3
A11
A9
Ø0
.01
4.7K
Data In
DACØ8
D/A
Vout 1
Vout 2
Bipolar Opt.
Socket
8
A
B

This circuit board was built using a hybrid, copper foil, wirewrap technique to minimize artwork layout time and to promote circuit design flexibility. The design was quite straightforward because all of the address, data and control lines were available at the 50-pin connector. However, a problem was initially encountered when the chip select pin on the VIA was connected to a microcomputer decoded chip select line. The completed circuit would not function even after repeated debugging attempts. It was later discovered that the microcomputer chip select line was decoded 100 nsec too late for correct decoding by the VIA chip. This problem was corrected by deriving the required chip select from a new 74LS138 address decoder added to an unused corner of the interface board. After this modification, the circuit performed as intended.

During a patient examination, this interface circuit latches data from each of the six flow qualifiers and passes the data to the microcomputer via a 6522 parallel input port. Flow data consists of a series of short pulses generated when the UA detects flow. The best way to capture these pulses was to have them set six set-reset latches which could be read and reset by the microcomputer program. The latches present a stable input to the parallel port without any pulse capture problems. During the time interval between the resetting and reading of the latches, any flow detected by a flow qualifier will cause its respective bit latch to be set.

Pulse-width to digital interface

The pulsed-Doppler ultrasonic arteriograph differs from continuous wave instruments because it has the ability to sample flow within small

volumes at various depths. The timing diagram of Figure 4 shows how the depth of the first sample gate is related to the pulse-width of the ΔT square wave. When the width of ΔT is increased, the time between the transmission of the ultrasound burst and the opening of the first sample gate is increased. By adjusting the width of ΔT with a potentiometer calibrated in tenths of a millimeter, the sample depth can be varied continually between 0 and 40 mm.

An interface circuit was designed to convert the pulse-width of ΔT to an 8-bit depth coordinate. The depth coordinate and the X-coordinate of the sample volume are used by the microcomputer to produce a depth view of the vessel. The circuit was constructed on a double-sided copper-foil circuit board as shown in Figure 13. A block diagram and timing diagram are shown in Figure 14 and a circuit schematic in Figure 15.

When power is applied, the circuit runs freely, storing new data with every cycle of ΔT. During a conversion cycle, the ΔT square wave is first input to a 7474 D-flip-flop which synchronize ΔT with the micro-computer clock. The ΔT output from that flip-flop is used to enable two 74161 4-bit ripple counters connected in series. When ΔT is high, the counter counts the 1 MHz microcomputer clock pulses. At the end of each count cycle, the falling edge of ΔT triggers monostable 1 (½ 74123) which generates a 100 nsec latch pulse. This pulse causes two 74175 D-latches to latch the counter outputs. The falling edge of this same latch pulse triggers monostable 2 (½ 74123) which generates a 100 nsec pulse that clears the 74161 counters. The outputs from the data latches are connected to two 74367 three-state buffers. When the board is

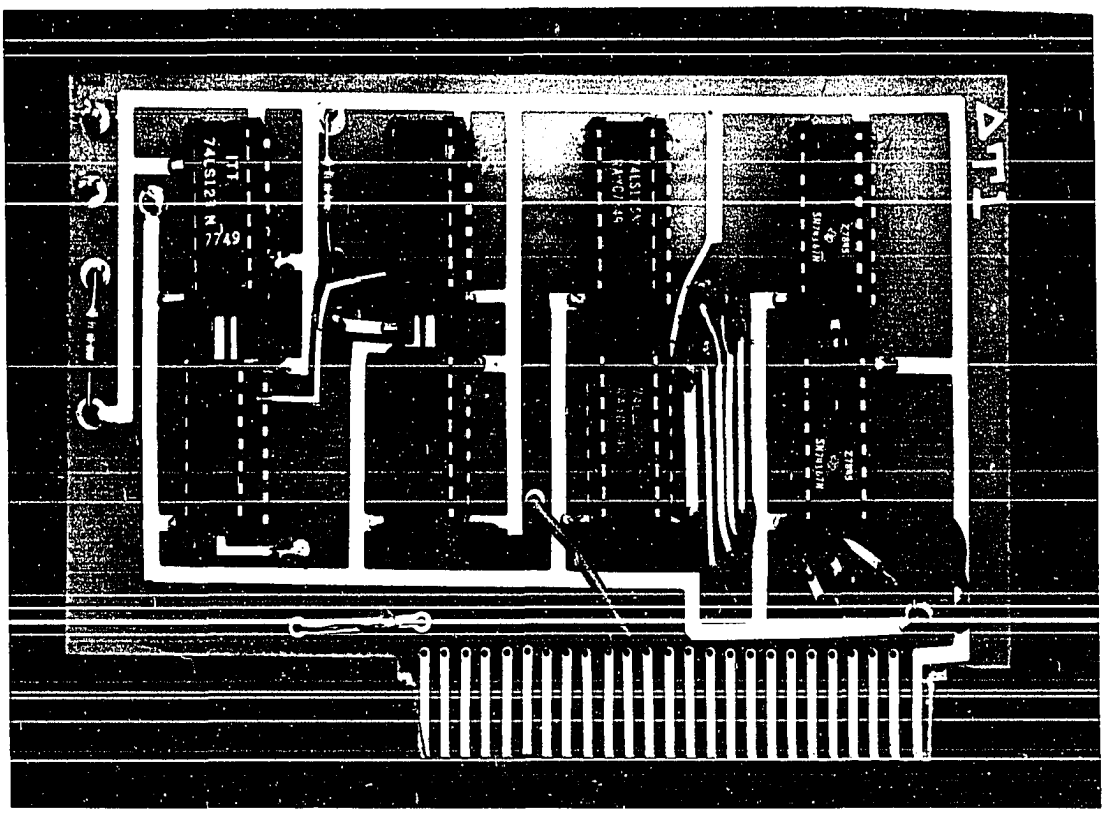

Figure 13. Photograph of pulse-width to digital interface board which computes the depth of the sample volume

Figure 14a. Block diagram of the pulse-width-to-digital interface circuit used to digitize the depth of the ultrasonic sample volume.

Figure 14b. Diagram explaining the timing events leading to the digitizing of the depth signal, ΔT.

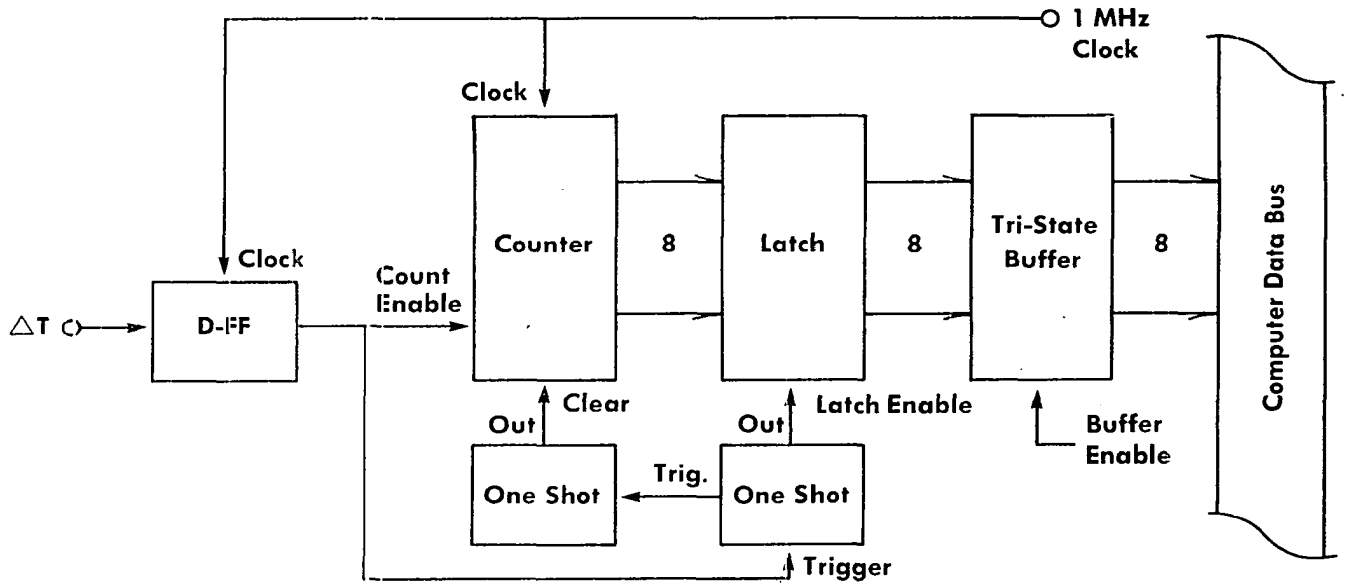
1 MHz
Clock
Clock
Clock
△T
D-FF
Count
Enable
Counter
8
Latch
8
Tri-State
Buffer
8
Computer Data Bus
Clear
Out
Latch Enable
Out
Buffer
Enable
One Shot
Trig.
One Shot
Trigger

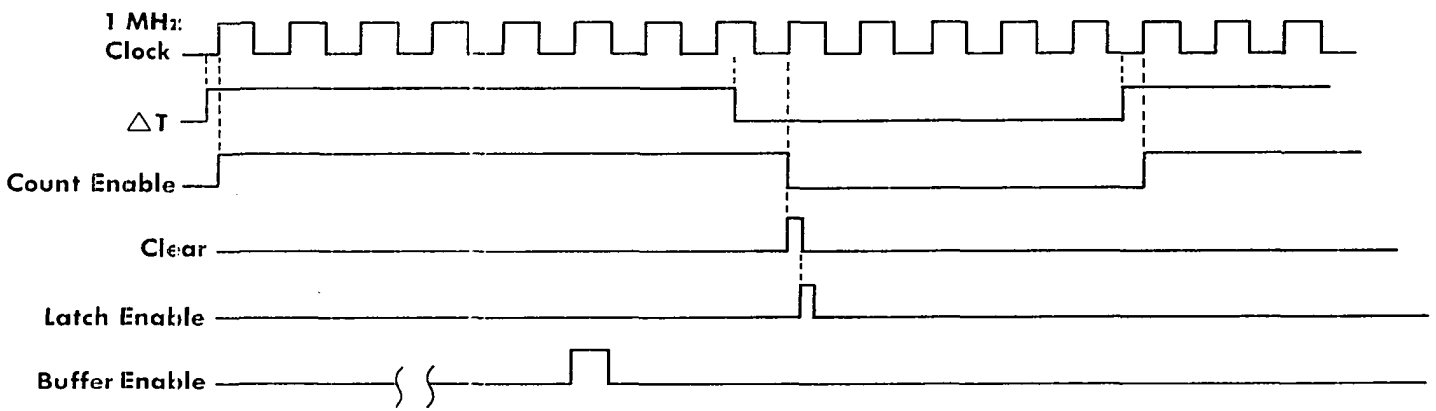
1 MHz
Clock
△T
Count Enable
Clear
Latch Enable
Buffer Enable

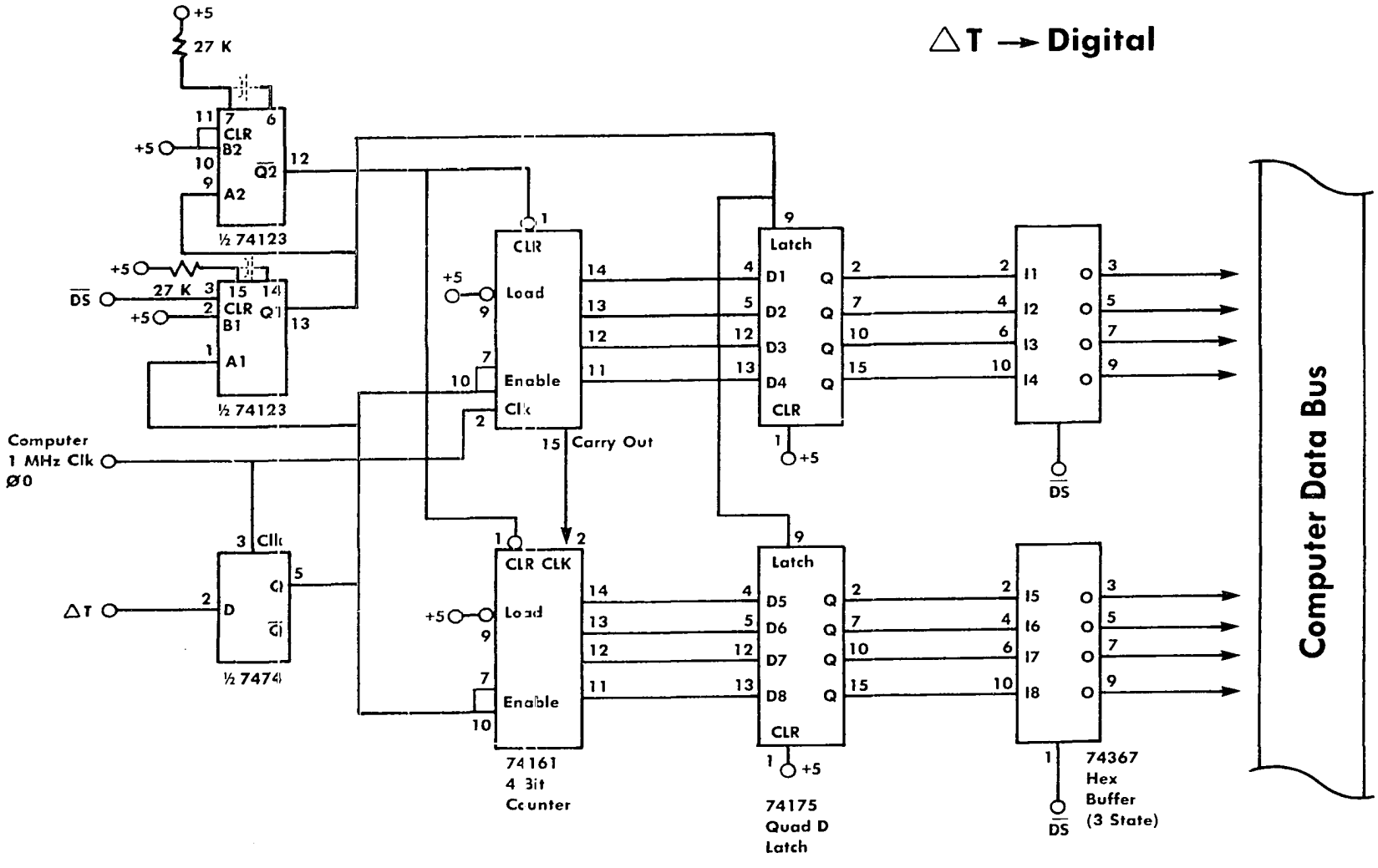

Figure 15. Circuit schematic of pulse-width-to-digital interface.

accessed during the execution of a program, the device select ($\overline{DS}$) line enables the buffers which place the depth data on the microcomputer data bus. During the 500 nsec period that the microcomputer is reading the latches, the data must not change. Data stability during this time is assured by using the $\overline{DS}$ line to inhibit the monostables.

To evaluate the circuit, the ΔT signal line from the UA was connected to the pulse-width-to-digital interface board. A ten-turn potentiometer on the UA calibrated in tenths of a millimeter was used to adjust the depth of the sample volumes. When the sample depth was varied from 0 to 40 mm, the pulse width of ΔT ranged from 0 to 67 μsec. Over this depth range, the converter circuit output from 1 to 67 counts for a resolution of 40 mm/ 67 counts or 0.6 mm/ count where each count represents a dot position on the video screen. This resolution was considered more than adequate for vessel imaging.

Imaging program

A program was written to input the x, y transducer coordinates via the A-D interface board, the depth of the sample volume via the pulse-width to digital converter board and the six bits of flow data via the parallel interface board. This data is used to produce images of the carotid arteries on a video screen. The arterial images are displayed as a plane view on the top two-thirds of the screen and a depth view on the bottom third.

The imaging program is interactive so the user can issue color change, erase screen, or save-image-on-disk commands from the keyboard while the program is executing. Furthermore, the program is able to

create arterial images in real-time without prolonging the time it takes to conduct a patient examination. In addition, the program will save the image on floppy disk for later retrieval and diagnosis by the physician.

For the following discussion, references should be made to the flow charts in Figures 16 and 17 or to the program listings in the appendix.

The imaging program begins by initializing variables, clearing the screen and loading the machine language subroutine, ML, from floppy disk. The program requests the user to enter the type of image to be generated and the user responds via the keyboard. The user can select a: 1) plane view, 2) depth view, or 3) plane and depth view. The program responds by asking for the patient's last name for later identification of the vessel image as it is stored on floppy disk.

The program sets the microcomputer into graphics made with 280 x 192 dot locations on the screen. As the patient examination begins, a POKE statement initiates the A-D conversions of the transducer X and Y position voltages. During the 1.25 msec required for conversion, the program uses a PEEK statement to read the flow information from the six gate latches. The presence of flow, as determined by each flow qualifier of the ultrasonic arteriograph, is represented as a binary 1 and the absence of flow is represented as a binary 0. The six bits of flow data are combined with two 0-bits and stored in an 8-bit memory location. For ease of display, the six flow bits are then separated and stored as six individual bytes of data by subroutine ML where a non-zero byte indicates the presence of flow at the depth of that sample gate. Subroutine ML also interrogates

Figure 16. Flowchart of the arterial imaging program written in BASIC.

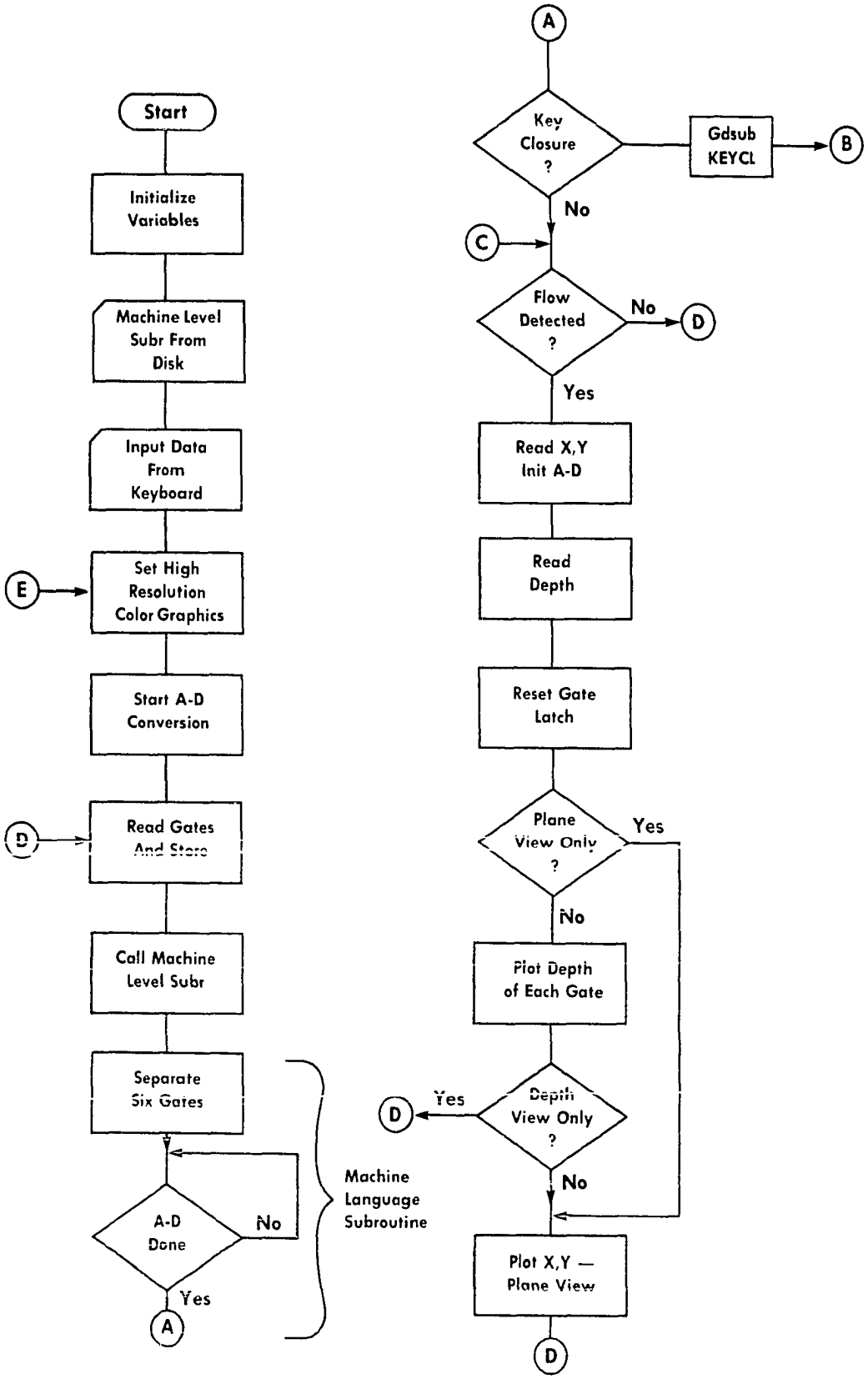
Start
Initialize Variables
Machine Level Subr From Disk
Input Data From Keyboard
E
Set High Resolution Color Graphics
Start A-D Conversion
D
Read Gates And Store
Call Machine Level Subr
Separate Six Gates
A-D Done
No
Yes
A
Machine Language Subroutine
A
Key Closure ?
Gdsub KEYCL
B
No
C
Flow Detected ?
No
D
Yes
Read X,Y Init A-D
Read Depth
Reset Gate Latch
Plane View Only ?
Yes
No
Plot Depth of Each Gate
Depth View Only ?
Yes
D
No
Plot X,Y — Plane View
D

Figure 17. Flow charts of subroutines called by the arterial imaging program when a keyboard command is entered by the examiner.

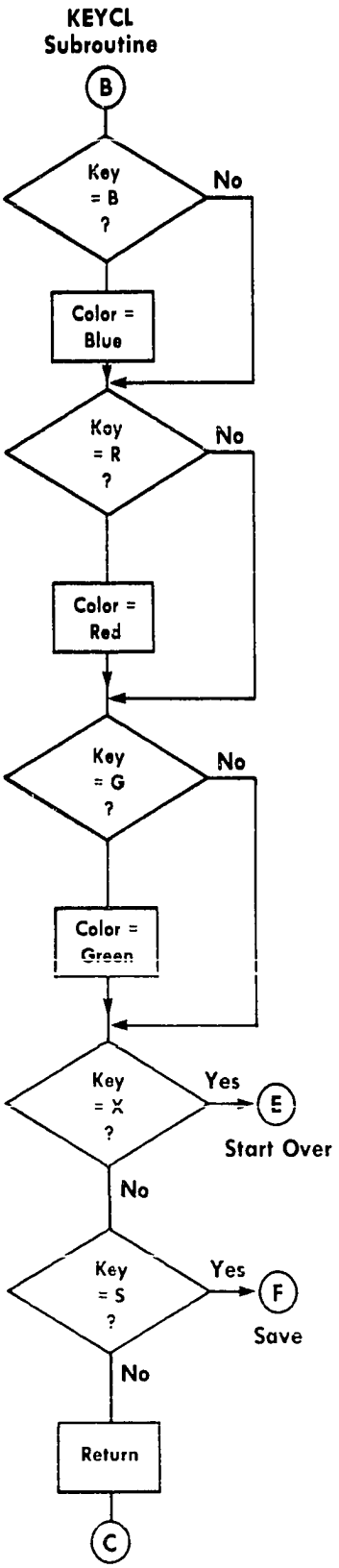
KEYCL
Subroutine
B
Key
= B
?
No
Color =
Blue
Key
= R
?
No
Color =
Red
Key
= G
?
No
Color =
Green
Key
= X
?
Yes
E
Start Over
No
Key
= S
?
Yes
F
Save
No
Return
C

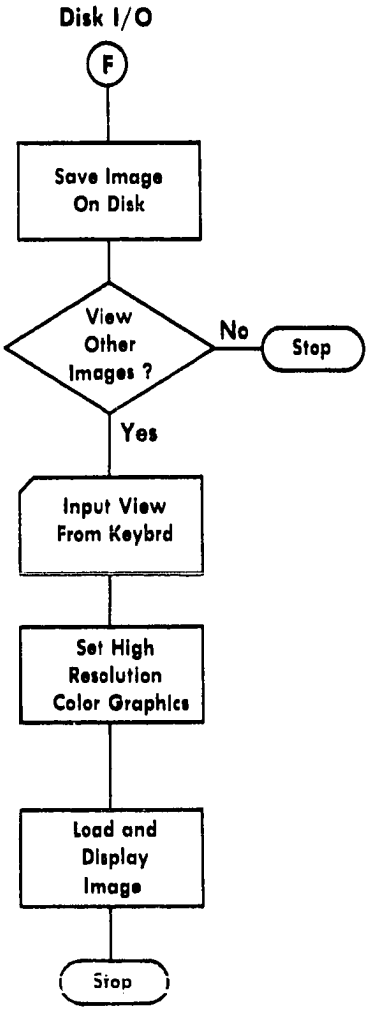
Disk I/O
F
Save Image
On Disk
View
Other
Images ?
No
Stop
Yes
Input View
From Keybrd
Set High
Resolution
Color Graphics
Load and
Display
Image
Stop

the A-D converters for conversion status, and if the conversion is not finished, it waits for completion then passes control back to the calling program.

When flow is detected by any of the flow gates, the transducer position coordinates are read from the X and Y A-D converters and a new A-D conversion is initiated. The program continues by using a PEEK statement to read the depth of the sample volumes from the pulse-width to digital interface board. At this point in the program, the X and Y transducer coordinates, the depth of the sample volume (Z), and flow data from each of the six sample gates are stored in memory. If flow was detected, the microcomputer places one dot in the plane view at its correct x, y position and up to six vertical dots in the depth view at appropriate x, z locations. Dot placement in both views takes place in a fraction of a second after which the program loops back, reads new flow and position data, and places more dots on the screen. A dot in the plane view indicates flow was detected by any number of the six sample gates at that x, y position. Six vertical dots in the depth view indicate that all six sample gates are detecting flow. If some of the vertical dots are not being lighted, their respective gates are not detecting flow. The examiner sees this and responds by adjusting the gate depth to determine if the vessel is within range of all the gates. If the depth is correct and some of the gates are still not detecting flow, then the vessel lumen is too narrow for all the range gates. Further vessel imaging is used to determine if the narrowing indicates tapering of the vessel or an occlusion. A partial vessel occlusion is shown in the image as a

narrowed flow channel which gradually expands to full width while a total occlusion is shown as an abrupt end of the vessel image.

At any time during the patient examination, the examiner may enter keyboard commands to: erase the image to start over; change the dot color; or stop the examination and save the image on floppy disk. Interactive communication, like this between the examiner and the microcomputer, is an important aspect of the imaging system. For example, when the examination begins, the ultrasonic probe is positioned on the neck and moved back and forth until the common carotid artery is located. This initial search often causes a noisy image which can be quickly erased by typing the "X" key on the microcomputer keyboard. The imaging program detects this key closure and jumps to the keyclosure (KEYCL) subroutine which determines which key was pressed then takes the appropriate action (see flowchart in Figure 17). At other times the examiner may wish to accentuate regions of the image by changing the dot color to blue, red, or green. This too can be accomplished by pressing the appropriate key on the keyboard. When the new color is set, new dots in both the plane and depth views have the same color. Thus, for example, when the internal carotid artery is located, a new color can be set to help identify the vessel in both the plane and depth views. In cases where separation between the carotid branches is slight, different colored dots prove to be a useful way of visually separating the branches in both views. Vessel regions which produce harsh Doppler signals characteristic of turbulence are identified with different colors. Physicians will find that color coding helps them quickly identify vessels and diseased regions

within vessels. At the conclusion of the examination, the "S" key can be pressed which causes the colored vessel image to be saved on floppy disk for later retrieval and diagnosis by the physician.

RESULTS AND CONCLUSIONS

A pulsed-Doppler ultrasonic arteriograph was interfaced to a microcomputer for the production of arterial images with three dimensions. The following sections describe the results of tests used to evaluate the accuracy and resolution of the new ultrasonic arteriograph along with examples of video images of the carotid bifurcation.

Resolution

Resolution, accuracy, stability and repeatability are important parameters of the new imaging system which were investigated and evaluated prior to using the instrument on human subjects. The video dots which compose the arterial images must be small enough and of sufficient quantity to produce a vessel image which has enough resolution to be diagnostically useful. However, it must be remembered that the lateral resolution of the image can be no better than the lateral resolution of the ultrasonic arteriograph which is on the order of 1mm.

The gain of the amplifiers had been adjusted so the plane view of the artery would be drawn on the top two thirds of the video screen. Resolution per dot was determined by moving the transducer through its maximum range in both the x and y directions, measuring the excursion and counting the number of dots on the screen. In the x-direction, the screen displayed 186 dots when the transducer was moved 130 mm for a resolution of 0.7 mm/ dot. In the y-direction, the screen displayed 97 dots when the transducer was moved 100 mm for a resolution of 1.0 mm/ dot. This resolution matches or exceeds the lateral resolution obtainable with the ultrasonic flowmeter.

In the orthogonal depth view, accuracy is determined in part by the accuracy of the potentiometer used to set the depth of the first sample gate and by the length of each sample volume. A ten-turn precision potentiometer with a dial calibrated in tenths of a millimeter is used to set the depth of the first sample gate. Range is determined by the time between the ultrasonic burst and the opening of the first gate and can be varied between 1 and 67 μsec (i.e. between 0 and 40 mm). The depth converter circuit outputs 1 to 67 counts over the 40 mm depth range for a resolution to the first sample gate of 40 mm/ 67 counts or 0.6 mm/ count. The value of the count determines the distance placed between the skin line and the blood vessel in the depth view. Vessel resolution in the depth view is limited by the length of the sample volumes. It was calculated that each gate has a minimum sample volume length of 1.9 mm. Thus to get all six gates within the vessel lumen the slant diameter must be >11 mm. In practice, the probe is inclined at a nominal angle of 45° relative to the vessel which effectively increases the viewed diameter 1/cos 45° or 1.4 times the actual vessel diameter. For example, six gates can sample flow within an 8 mm vessel allowing diameter reductions in 15% increments to be detected. Five sample gates can detect flow within a 6 mm diameter vessel allowing diameter reductions in 20% increments to be detected and so on for fewer gates.

Accuracy and Repeatability

The stability and precision of the circuit components used in the instrument determine how accurately the dots trace the movements of the

transducer. Thermal drift plays a large part in the stability of the components and the repeatability of the tracings.

Position accuracy is in part determined by two "precision" potentiometers, with 0.25 percent linearity, which produce a varying dc voltage as a function of the shaft angle. These potentiometers are connected to the positioning arm and define the x, y arterial coordinates for the plane view and the x coordinate for the depth view. The position voltages are amplified and input to the 8-bit A-D converters whose conversion stability is guaranteed by the manufacturer to be within ± ½ the least significant bit (LSB) over the specified temperature range of the IC. A precision voltage regulator provides a highly stable reference voltage for the A-D converter in order to maintain the ± ½ LSB accuracy.

The stability and repeatability of the imaging system was measured by the microcomputer in two tests. Prior to the tests the instrument was allowed to warm-up for 30 minutes. Stability of the transducer positioning system was determined by placing the transducer positioning arm in a fixed position while using the microcomputer to control the timing of the A-D converter which digitized the position voltages once every second for 30 minutes (A-D conversions take place in 1.25 msec). During the test, the microcomputer displayed out the x and y position coordinates on the video screen. With this test, the count was found to be highly stable, but it also tended to decrease monotonically over the 30 minutes due to thermal drift. At the end of the test, the microcomputer printed out the minimum and maximum readings and the time they

occurred. It was found that both converters drifted to produce a change of -4 counts over the 30 minute test. While this amount of drift is undesirable, it is felt that the short term conversion stability is more important since the examiner never retraces the path of the transducer after a long time delay.

In the next test, the transducer was moved back and forth within a metal track over a fixed distance of 6 cm, while the position coordinates of the transducer were being read by the microcomputer. A program was written which took the derivative of the position as a function of time. Transducer position was plotted on the screen in the vertical (y) direction while the horizontal position of the dots was incremented every time the transducer changed directions (i.e. when the position derivative changed sign). By moving the transducer 60 times between end supports of the track, a solid rectangle was drawn on the screen. The repeatability of the transducer position was determined by observing how straight the top and bottom sides of the rectangle were. If it is assumed that the transducer reached the track limits each time, the repeatability was found to be within one count each time the transducer was moved. As demonstrated by this test, repeatability is sufficient to produce good quality arterial images.

Vessel imaging

Healthy volunteers were used for each of the vessel imaging procedures to be described. Since the new system was not proven, it was felt that a baseline or standard had to be developed which could be used to evaluate the operation of the instrument prior to using it on patients with diseased vessels.

In the first trial, a plane view alone was drawn on the video screen during a normal ultrasonic examination. A photograph of the video image is shown in Figure 18. The quality of the video image was not as good as the CRT image but still provided a good outline of the vessel lumen. Poorer resolution was due in part to the fast movements of the transducer which were averaged by the A-D converters. In later experiments, the examiner slowed his movement of the transducer and better resolution was obtained.

With the success of the plane view, both plane and depth views were produced in the remainder of the trials. The images were made with red, green and blue dots representing different regions of the vessel in both the plane and depth views. This programming function improves the identification of the vessel branches between the two views.

Depth views are unique and can not be compared to the images produced by any other ultrasonic arteriograph; however, evaluation can be made based on the resolution required for diagnosis. Examples of plane and depth views of normal carotid arteries are shown in Figures 19 and 20. To produce these views, the examiner must adjust the depth of the range gates smoothly to keep the sample volumes within the arterial lumen and to maintain a smooth edge on the image of the vessel. Gate spacing must be set so the outside gates sample flow along the vessel wall. Otherwise, the depth view will not correctly depict the lumen boundaries. In cases where the angle between the vessel axis and the ultrasonic beam becomes more acute, the vessel will appear wider since the slant diameter and gate spacing will increase proportionally. However, since absolute gate

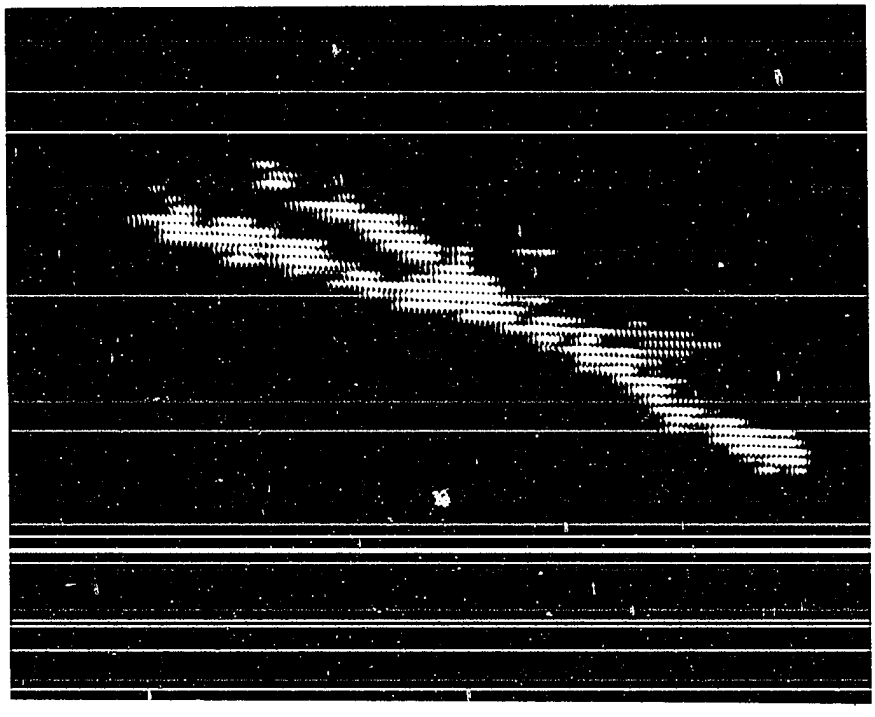

Figure 18. Plane view of a carotid bifureation produced with the new imaging system

Figure 19. Plane and depth view of a normal carotid bifurcation. The line in the middle represents the skin at zero sample depth.

Figure 20. Plane and depth view of a normal carotid bifurcation. The bottom branch in both views is the internal carotid artery.

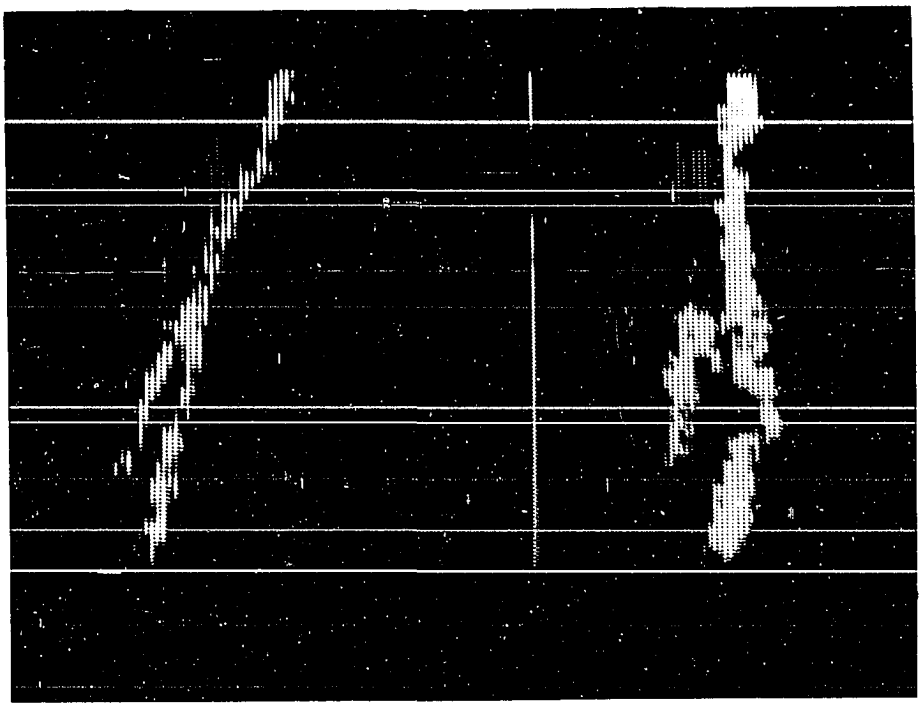

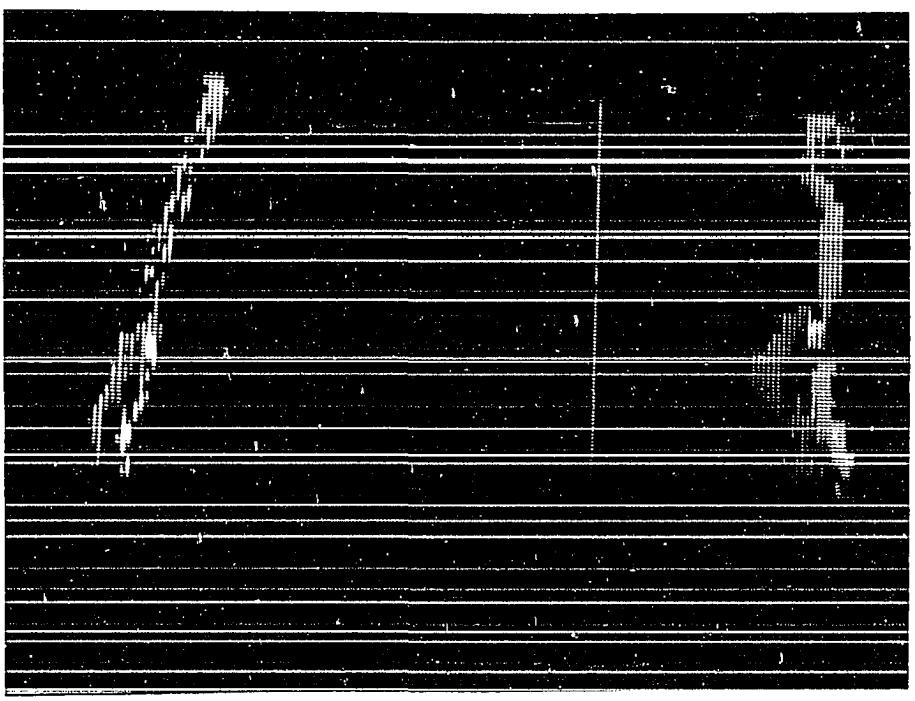

spacing is not shown in the depth view. The true vessel diameter will not be known. Additional problems are encountered when the internal and external branches of the common carotid are close together. However, if the external carotid is drawn in one color and the internal carotid in another color, the vessels can be separated in the image. However, when the two branches are at the same depth, the branch imaged last will hide the first branch image. This image is geometrically correct since the depth view is actually a projection of the vessels onto a depth plane where surfaces nearest to the transducer will hide surfaces lying behind. The best way to surmount this problem is to approach the vessels from a different angle.

Even with the problems alluded to in the preceding paragraph, the depth view, if interpreted by a knowledgeable individual, will provide valuable information about the depth of the vessel and about which gates were detecting flow at that depth.

Conclusion

The arterial imaging system performed as planned, producing plane and depth views of the carotid arteries. Tests determined that the stability and accuracy of the electronic components which make up the system were satisfactory. Image resolution in the plane view was approximately 1 mm^2 per dot position, which yields good quality outlines of the vessel lumen. Vessel depth was displayed in 0.67 mm increments, which is sufficient for accurate depth measurements. Individual dots for each of the six sample gates were used to produce depth views of the arteries. Resolution of the flowmeter limits the resolution across the vessel to

1.9 mm per gate in the depth direction. In an 8 mm carotid artery, this permits all six gates to lie within the lumen of the vessel when the probe is inclined at 45^{o} relative to the vessel axis. Thus, for an 8 mm vessel, the depth view can be used to estimate diameter reductions in increments of 15%. This depth resolution is a dramatic improvement over previous instruments which are not capable of any display resolution in the depth direction.

Future tests on patients with normal and diseased vessels will be used to further evaluate this new imaging system.

SUMMARY

The project described in this dissertation involved the design and development of a microcomputer-aided, pulsed-Doppler ultrasonic arteriograph used to image the extracranial bifurcation of the carotid arteries. This new system uses the position coordinates of detected blood flow to produce two orthogonal views of the carotid arteries on a video screen. The arteries are displayed as a plane view and a depth view which provide the physician with three dimensional spatial information that can be used to better diagnose atherosclerotic occlusive disease. Imaging the carotid arteries with three dimensions represents a significant new technique that produces additional diagnostic information that was heretofore unavailable with non-invasive techniques.

The imaging system incorporates a microcomputer with high resolution color graphics capability that was interfaced to a Hokanson ultrasonic arteriograph (UA). Microcomputer interface circuits were designed and built to digitize transducer position, sample depth and blood flow signals produced during an examination. An interactive microcomputer program was written to analyze the examination data and produce two views of the carotid bifurcation on a video screen. The plane view is similar to a lateral view obtained with X-rays, while the depth view is similar to an anterior-posterior X-ray view. These new images are capable of better than 1 mm resolution, meaning that a vessel diameter change of less than 1 mm can be detected.

Prior to the development of this new system, single two-dimensional vessel images were used to estimate the size of a three-dimensional

stenosis. This estimation introduces errors if the stenosis is asymmetrical and not in the plane being imaged. These errors reduced the physicians' confidence in ultrasound causing them to prescribe more elaborate tests.

The new imaging system improved the diagnostic accuracy of ultrasound by producing two orthogonal views of the carotid bifurcation which are used to better estimate the arterial lumen reduction caused by a stenosis. These arterial views also reduce the number of false positive and false negative examinations caused by misinterpretation of the image due to the lack of a depth view.

RECOMMENDATIONS FOR FURTHER STUDY

This present study exemplifies how present generation microcomputers can be utilized to enhance the diagnostic capabilities of medical instrumentation. Microcomputers are low enough in cost that they can be designed into many instruments to improve their capabilities and increase their functions. However, microcomputers have drawbacks too; among other things, they are slow when it comes to repetitive computations and time consuming to program. Careful consideration should be given to incorporating a microcomputer into an instrument at the chip, board or system level.

Ultrasonic diagnosis is technologically still in its infancy. Researchers are continually advancing the forefront of knowledge at a rapid pace. For example, researchers are currently experimenting with spectral analysis of Doppler flow signals using the new Fast Fourier Transform computers to improve the diagnositc capabilities of ultrasound. Others are using a combination pulse-echo and pulse-Doppler ultrasound system to image diseased arteries.

In line with this project, it is planned to use the microcomputer to control the searching and tracking of the vessel under examination. The program will also automatically oscillate the sample volume between the vessel walls to improve the resolution of the image in the depth view while also reducing the burden of the examiner. In addition, the ultrasonic arteriograph will be redesigned to improve the depth resolution by increasing the number of sample gates from six to eight.

Vascular research, like research in general, is very rewarding if the investigator uses a little imagination, careful planning, outside funding, many hours in the laboratory and many more hours analyzing and writing the results for publication and presentation. If the investigator can master these few rules, he or she will be successful.

RESEARCH APPROVAL

This research project has been approved by the Human Subjects Research Committees of: Iowa State University, Ames; Southern Illinois University School of Medicine, Springfield; and Saint John's Hospital, Springfield, Illinois.

BIBLIOGRAPHY

Baker, D. W. 1970. Pulsed ultrasonic Doppler blood-flow sensing. IEEE Transactions on Sonics and Ultrasonics SU-17 (3):170-185.

Baker, D. W., S. L. Johnson and D. E. Strandness. 1974. Prospects for quantification of transcutaneous pulsed Doppler techniques in cardiology and peripheral vascular disease. In R. S. Reneman, ed. Cardiovascular applications of ultrasound. American Elsevier Publishing Co., Inc., New York. 462 pp.

Caro, C. G., J. M. Fitzgerald, and R. C. Schroter. 1971. Atheroma and arterial wall shear-observation, correlation and proposal of a shear dependent mass transfer mechanism for atherogenesis. Proceedings of the Royal Society of London B, 177:109-159.

Francis, C. C. 1959. Introduction to Human Anatomy. Third edition. C. V. Mosby Co., St. Louis, Missouri. 548 pp.

Franklin, D. L., D. W. Baker and R. M. Ellis. 1959. A pulsed ultrasonic flowmeter. IRE Transactions in Medical Electronics 6:204.

Franklin, D. L., W. Schlegel, and R. F. Rushmer. 1961. Blood flow measured by Doppler frequency shift of backscattered ultrasound. Science 134:564-565.

Fry, D. L. 1969. Certain histological and chemical responses of the vascular interface to acutely induced mechanical stress in the aorta of the dog. Circulation Research 24:93.

Hokanson, D. E., D. Mozersky, D. S. Sumner and D. E. Strandness, Jr. 1971. Ultrasonic arteriograph: A new approach to arterial visualization. Biomedical Engineering 6:420.

Kalmus, H. P. 1954. Electronic flowmeter system. Review of Scientific Instruments 25 (3): 201-206.

Kato, K., M. Motomiya, T. Izumi, Z. Kaneko, J. Shiraishi, H. Omizo, and S. Nakano. 1965. Linearity of readings on ultrasonic flowmeter. International Conference on Medical Electronics and Biological Engineering, Tokyo. Digest of Papers for Scientific Program 6:284-285.

Keller, H. M., W. E. Meier, M. Anliker, D. A. Kumpe. 1976. Noninvasive measurement of velocity profiles and blood flow in the common carotid artery by pulsed Doppler ultrasound. Stroke 7(4):370-377.

Lloyd, E. A. 1967. Energy measurement. In B.Brown and D. Gordon, eds. Ultrasonic techniques in Biology and Medicine. Thomas Publishing Co., Springfield, Illinois. p. 52.

McLeod, F. D. 1967. A directional Doppler flowmeter. Digest of the 7th International Conference in Medical and Biological Engineering 7:213.

McLeod, F. D. 1974. Multichannel pulse Doppler techniques. Pages 85-107 in R. S. Reneman, ed. Cardiovascular applications of ultrasound. American Elsevier Publishing Co., Inc., New York.

Morris, R. L., M. B. Histand, and C. W. Miller. 1973. The resolution of the ultrasound pulsed Doppler for blood velocity measurements. Journal of Biomechanics 6:701-710.

Mozersky, D. J. and D. E. Hokanson, D. W. Baker, D. S. Sumner, and D. E. Strandness. 1971. Ultrasonic arteriography. Archives of Surgery 103:663-667.

Nippa, J. H., D. E. Hokanson, D. R. Lee, D. S. Sumner, D. E. Strandness, Jr. 1975. Phase rotation for separating forward and reverse blood velocity signals. IEEE Transactions on Sonics and Ultrasonics SU-22(5):340-346.

Peronneau, P. A. and F. Leger. 1969. Doppler ultrasonic pulsed blood flowmeter. International Conference in Medical and Biological Engineering and 22nd Annual Conference on Engineering in Medicine and Biology, session 10-11, Chicago.

Reid, J. M. and M. P. Spencer. 1972. Ultrasonic Doppler techniques for imaging blood vessels. Science 176:1235-1236.

Reneman, R. S. and M. P. Spencer. 1974. Difficulties in processing of an analogue Doppler flow signal; with special reference to zero-crossing meters and quantification. In R. S. Reneman, ed. Cardiovascular applications of ultrasound. American Elsevier Publishing Co., Inc., New York. 462 pp.

Roberts, B., W. H. Hardesty, H. E. Holling, M. Reivich, and J. F. Took. 1964. Studies on extracranial cerebral blood flow. Surgery 56:826.

Russell, J. B., D. S. Sumner, W. M. Hajjar, D. E. Ramsey and R. D. Miles. 1979. Pulsed Doppler imaging of the carotid bifurcation: The most sensitive non-invasive method for diagnosing extracranial arterial disease. (Submitted for publication)

Satomura, S. 1959. A study of the flow patterns in peripheral arteries by ultrasonics. Journal Acoustical Society of Japan 15:151-158.

Spencer, M. P., E. C. Brockenbrough, D. L. Davis and J. M. Reid. 1977. Cerebrovascular evaluation using Doppler C-W ultrasound. Ultrasound in Medicine 3B:1291-1310.

Thompson, J. E. 1975. Cerebrovascular insufficiency. In W. F. Barker, ed. Peripheral artery disease. W. B. Saunders Co., Philadelphia. 503 pp.

Tsai, F. Y., B. E. Morgan, and D. F. Young. 1971. Effects of stenosis geometry on flow through a locally constricted tube. Iowa State University Engineering Research Institute Report No. 99904.

Voss, D. J., P. C. Petersen, G. D. Mahler, and F. E. Barber. 1977. A microprocessor-based blood flow display for pulsed Doppler systems. In D. White and R. Brown, eds. Ultrasound in medicine. Vol. 3B. Plenum Publishing Co., New York.

White, D. N. and G. R. Curry. 1978. A comparison of 424 bifurcations examined by angiography and Doppler echoflow. In D. White and E. A. Lyons, eds. Ultrasound in medicine. Vol. 4. Plenum Publishing Co., New York.

ACKNOWLEDGEMENTS

I wish to express my sincere appreciation to the many people who gave their support and advice throughout this research project.

Special thanks go to Dr. D. L. Carlson and Dr. A. V. Pohm for serving as my major professors. They kept me from straying too far from my original proposal and offered many helpful suggestions and criticisms. I am also grateful to Dr. D. F. Young who taught me the fundamentals of research and introduced me to hemodynamics five short years ago.

Thanks to Dr. Cholvin, Dr. Camp and Dr. Grosvenor for serving on my graduate committee. Dr. Cholvin served on both of my graduate committees which speaks for the respect that I have for him. Drs. Camp and Grosvenor willingly and graciously gave me technical support in the areas of microcomputers and computer programming.

I am grateful to my family for their encouragement, support and aid they gave me during my college career. Special thanks and love go to my wife, Diane, who showed her devotion by giving clerical assistance and offering constructive criticisms during all stages of this research project.

I would also like to thank Dr. D. S. Sumner, James Russell, and Dr. D. E. Ramsey of the SIU Department of Surgery for their ideas, assistance and encouragement during the past year. I am also grateful to Miss Peggy Soeldner for offering to type the final draft of this dissertation when everybody else was too busy.

APPENDIX: PROGRAM LISTINGS

```
 1 REM -- BASIC PROGRAM, MARCH 19, 1979
 2 REM -- HIGH RESOLUTION GRAPHICS PROGRAM
 3 REM -- TO GENERATE IMAGES OF ARTERIES
 4 REM -- FROM DATA PRODUCED BY AN ULTRA
 5 REM -- SONIC ARTERIOGRAPH
10 LOMEM: 25000
12 REM -- SETS LOWEST MEMORY LOCATION USED
15 D$ = CHR$ (4): REM -- DISK CONTROL CHAR.
20 ONERR  GOTO 3000
25 HOME
30 INPUT "FIRST RUN (Y,N) ?"; U$
40 IF U$ = "N" THEN 70
50 PRINT D$; "BLOAD INPUT, D2, V254"
55 REM -- MACHINE LANGUAGE SUBROUTINE
60 POKE -- 15614,0: REM  INIT VIA B-IN
70 HOME: HTAB 10: VTAB 10: PRINT "SELECT 1, 2, 3, OR 4"
80 PRINT: HTAB 14: PRINT "1 PLANE VIEW"
85 HTAB 14: PRINT "2, DEPTH VIEW"
90 HTAB 14: PRINT "3, PLANE AND DEPTH VIEW"
92 HTAB 14: PRINT "4, SELECT IMAGE ON DISK"
95 INPUT Q: IF Q > 4 OR Q < 1 THEN 70
98 IF Q = 4 THEN 1010
100 INPUT "PATIENTS LAST NAME ?"; P$
110 HGR2: HCOLOR = 1: REM RED
115 POKE -- 16205,0: REM -- INIT A/D CONVERSION
120 G = PEEK (- 15616) - 128: POKE 24800, 0
125 CALL 24576: REM -- SEPARATE GATES AND WAIT FOR A/D TO FINISH
140 KEY = PEEK (- 16384): POKE -  16368,0
145 REM -- READ KEYBOARD FOR COMMAND
147 IF KEY > 128 THEN GOSUB 2000
```

```
165 IF G = 0 THEN 120: REM  NO FLOW DETECTED
170 Y = PEEK (- 16207): X = 255  - PEEK (- 16206)
180 IF Y > 159 THEN Y = 159: YLIMIT
182 POKE  - 16205,0: REM  INIT A/D CONVERSION
185 D = 0
190 FOR I = 1 TO 5:D = D + (60 - PEEK (- 16176)):
    NEXT: D = INT (D/3)
200 POKE  - 15604,224: POKE  - 15604,192
205 REM  RESET GATE LATCH
210 IF Q = 1 THEN 290
215 REM
220 REM-- ROUTINE TO PLOT DEPTH VIEW
230 HPLOT X,100: REM -- SKIN LINE
240 FOR I = 0 TO 5: IF PEEK (24806 - 1) = 0 THEN 260
250 :: HPLOT X,100 + D + 1
260 NEXT
270 IF Q = 2 THEN 120
280 REM -- ROUTINE TO PLOT PLANE VIEW
290 HPLOT X,Y
300 GOTO 120
1000 PRINT D$; "BSAVE"; P$; Q;", A$4000, L$2000, V4, D1"
1010 TEXT: D$ = CHR$ (4)
1020 HTAB 15: PRINT "DO YOU WANT TO VIEW ANY OF THE IMAGES
     ON DISK (Y/N)?"
1030 INPUT Q$: IF Q$ = "N" THEN END
1040 INPUT "WHAT VIEW SELECTION? (1, 2 OR 3)"; Q
1050 INPUT "PATIENTS LAST NAME?"; P$
1060 HGR2
1070 PRINT D$; "BLOAD"; P$; Q;", V4, D1"
1080 END
2000 IF KEY = 194 THEN HCOLOR = 2: REM BLUE = B
2010 IF KEY = 210 THEN HCOLOR = 1: REM RED = R
2015 IF KEY = 199 THEN HCOLOR = 6: REM GREEN = G
```

```
2020 IF KEY = 216 THEN 110
2025 IF KEY = 211 THEN 1000: REM  SAVE = 5
2030 RETURN
3000 TEXT: PRINT "ERROR, TYPE 'RUN' TO START OVER"
3050 END
```

SUBROUTINE ML March 17, 1979

Address	1st	2nd	3rd	Symbol	Instruction	Comments
6000	A9	02		Gate	LDA #$02	One bit for
6002	8D	DF	60		STA $60DF	Anding with gates
6005	A2	06			LDX #06	Loop counter
6007	AD	DF	60	Repeat	LDA $60DF	Flow gates loaded
60DA	2D	EO	60		AND $60ED	Bit check for flow
600D	9D	EO	60		STA$60EO,X	IF ≠ 0 then
6010	OE	DF	60		ASL $60DF	Flow is present
6013	CA				DEX	Decrement counter
6014	DO	F1			BNE $6007	Repeat
6016	AD	BO	CO	ADC	LDA $COBO	A-D status loaded
6019	29	CO			AND #$CO	Mask B7, B6
601B	DO	F9			BNE$6016	Not done
601D	60				RTS	A-D done

DATA LOCATIONS IN R/W MEMORY

Address	
60DF	Single bit for ANDing with flow data
60EO	GSUM - flow bit
60E1	G6 - flow bit
60E2	G5 - flow bit
60E3	G4 - flow bit
60E4	G3 - flow bit
60E5	G2 - flow bit
60E6	G1 - flow bit
.	
.	
.	
60ED	Flow data